N

NATIONAL AERONAUTICS AND SPACE ADMINISTRATION

Technical Report 32-1269

The Mariner Venus 67 Magnetic Field Control Program

Joseph G. Bastow

JET PROPULSION LABORATORY
CALIFORNIA INSTITUTE OF TECHNOLOGY
PASADENA, CALIFORNIA

April 15, 1968

NATIONAL AERONAUTICS AND SPACE ADMINISTRATION

Technical Report 32-1269

The Mariner Venus 67 Magnetic Field Control Program

Joseph G. Bastow

Approved by:

W. S. Shipley, *Manager*
Environmental Requirements Section

JET PROPULSION LABORATORY
CALIFORNIA INSTITUTE OF TECHNOLOGY
PASADENA, CALIFORNIA

April 15, 1968

TECHNICAL REPORT 32-1269

Prepared Under Contract No. NAS 7-100
National Aeronautics & Space Administration

Contents

Tables

Contents (contd)

Tables (contd)

Figures

Abstract

Magnetic control efforts on *Mariner* Venus 67 were limited to reducing and stabilizing the magnetic field of existing hardware and to obtaining more meaningful information on the magnetic condition of the hardware than had been obtained in the *Mariner* Mars 1964 program. All type approval hardware was magnetized and demagnetized and, if no adverse demagnetization effects were observed, all flight hardware was demagnetized to erase the effects of environmental testing and to stabilize and reduce the magnetic field. A simple facility was erected in the spacecraft assembly area at JPL where assemblies and subassemblies could be magnetically mapped and magnetized or demagnetized. A similar, but smaller, facility was erected at Cape Kennedy to maintain the spacecraft magnetic integrity until launch. Magnetic mapping data were processed by computer to provide the magnetic field components of the extrapolated field in spacecraft coordinates at the spacecraft magnetometer sensor. These field components were summed and compared with the mapped field of the complete spacecraft.

While this program succeeded in reducing the spacecraft magnetic field, it did not resolve the problem of magnetic stability. Magnetic stability remains intimately related to the amount and type of magnetic material in the hardware, while the total spacecraft field is more dependent on placement and orientation of hardware on the spacecraft. The results of this program clearly demonstrate that a spacecraft can have a low total field and yet be made up of many subassemblies with very large, and potentially unstable, magnetic fields.

The results of the technique of summing the subassembly fields, when compared with the total spacecraft mapped field, show significant correlation and provide insight into the effect of removing or adding a single item of hardware on the total spacecraft field. Additional work remains on the interpretation of irregular, nonsinusoidal mapping results to improve the correlation between these summed and mapped fields.

The *Mariner* Venus 67 Magnetic Field Control Program

I. Introduction

The *Mariner* Venus 67 program, as originally conceived, was to take hardware and a spacecraft designed for travel away from the sun and to modify them to the extent necessary for travel toward the sun. Because the primary mission was to obtain scientific information that would complement or extend the results obtained by *Mariner* Venus 1962, essentially the same experiments were to be carried by the spacecraft on its flight to Venus. A magnetometer was, again, one of the experiments to be flown on the spacecraft.

The magnetic field experiment created a need for a low and stable ambient field caused by the spacecraft. With the added constraint that the *Mariner* Mars 1964 hardware would be employed, with necessary modifications for a Venus flight, magnetic control efforts were faced with a dilemma. Most of the *Mariner* Mars hardware failed to fully satisfy the rather stringent magnetic requirements. With very little opportunity to eliminate magnetic materials in this hardware, other means were necessary to improve the magnetic quality of the spacecraft.

II. Magnetic Control Plan

A. Development of the Plan

Initially, a magnetic control plan was prepared calling for an investigation of spacecraft hardware magnetic stability and a more extensive and thorough magnetic evaluation program than that for the *Mariner* Mars 1964 project. Because of budgetary limitations, it was necessary to curtail the desired program. The magnetic control plan, as it finally evolved for the *Mariner* Venus program, was a compromise based on severe hardware constraints and both schedule and budgetary limitations. All stray field or current loop tests, except those on the solar panels and the completely assembled spacecraft, which were essential to the evaluation of the magnetic field reported by the spacecraft in flight, were to be omitted.

Because of the success in reducing the magnetic field of the *Mariner* Mars Proof Test Model (PTM) by demagnetization, this technique was selected as the principal effort on the *Mariner* Venus 67 shown in Figs. 1 and 2. This procedure would reduce the magnetic field and, hopefully, stabilize it by erasing the effects of the vibration testing. It was expected that, as a result of vibration

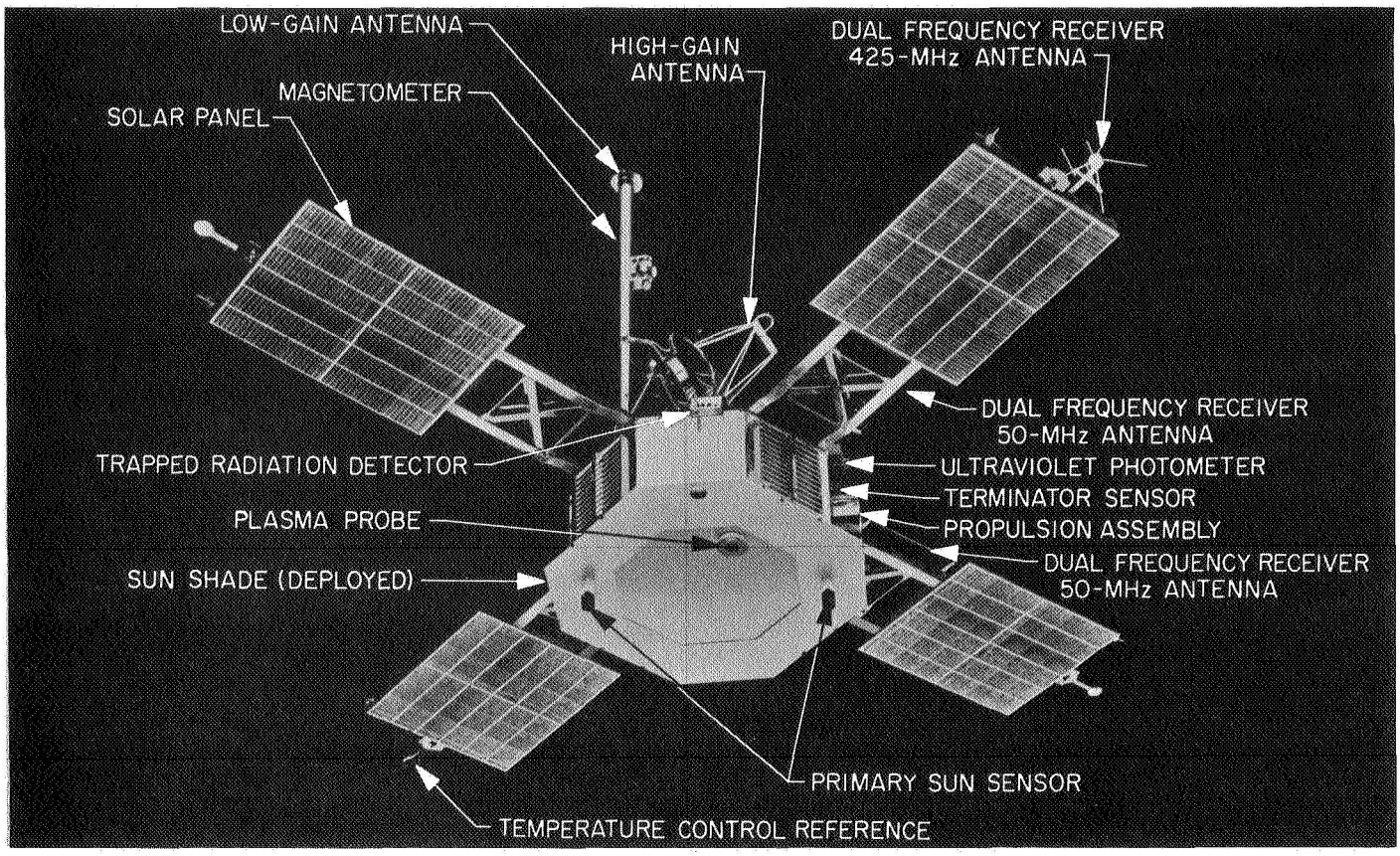

Fig. 1. *Mariner* Venus 67

View of solar illuminated side of spacecraft. Solar panels are attached at Bays 1, 3, 5, and 7 proceeding counterclockwise from panel at lower right

testing on a shaker with a 5- to 10-Oe field, hardware would acquire a much higher residual magnetization than as a result of vibrations in the earth's field during launch. Consequently, the magnetic stability of the hardware would probably be poorer if it were not demagnetized prior to launch.

The Project Office had set the goal that "the magnetic quality of the spacecraft (*Mariner* Venus 67) should be at least equal to that of *Mariner* Mars 1964. An attempt should be made to improve this quality with techniques compatible with the schedule and fiscal restraints." Consistent with this goal, any contemplated changes in hardware design were to be reviewed to determine their effect on the magnetic quality of hardware. This was accomplished by consultation with each of the hardware cognizant engineers and by review of each of the Engineering Change Requests (ECRs) approved by the spacecraft system engineer.

Next, a comprehensive magnetic evaluation was to be made on type approval (TA) or prototype hardware to verify the effectiveness of demagnetization, to ensure that no adverse effects would result from demagnetization, and to obtain information on the magnetic stability of the hardware. Finally, if demagnetization was found effective and safe, the flight hardware would be demagnetized.

Demagnetization of flight hardware was to be accomplished as late in the schedule as possible, at least after all vibration and shock testing. Although the *Mariner* Mars PTM had been successfully demagnetized as a complete spacecraft, except for solar panels, it was believed that more effective demagnetization would be obtained if the ambient field could more effectively be reduced over the volume of the hardware. A larger facility to accomplish this demagnetization at the system level was not considered feasible; therefore, it was decided to demagnetize the hardware at the assembly level as much as possible. This also was compatible with demagnetization at the latest possible time, because the hardware would be available for demagnetization at this level during the course of the final spacecraft disassembly and

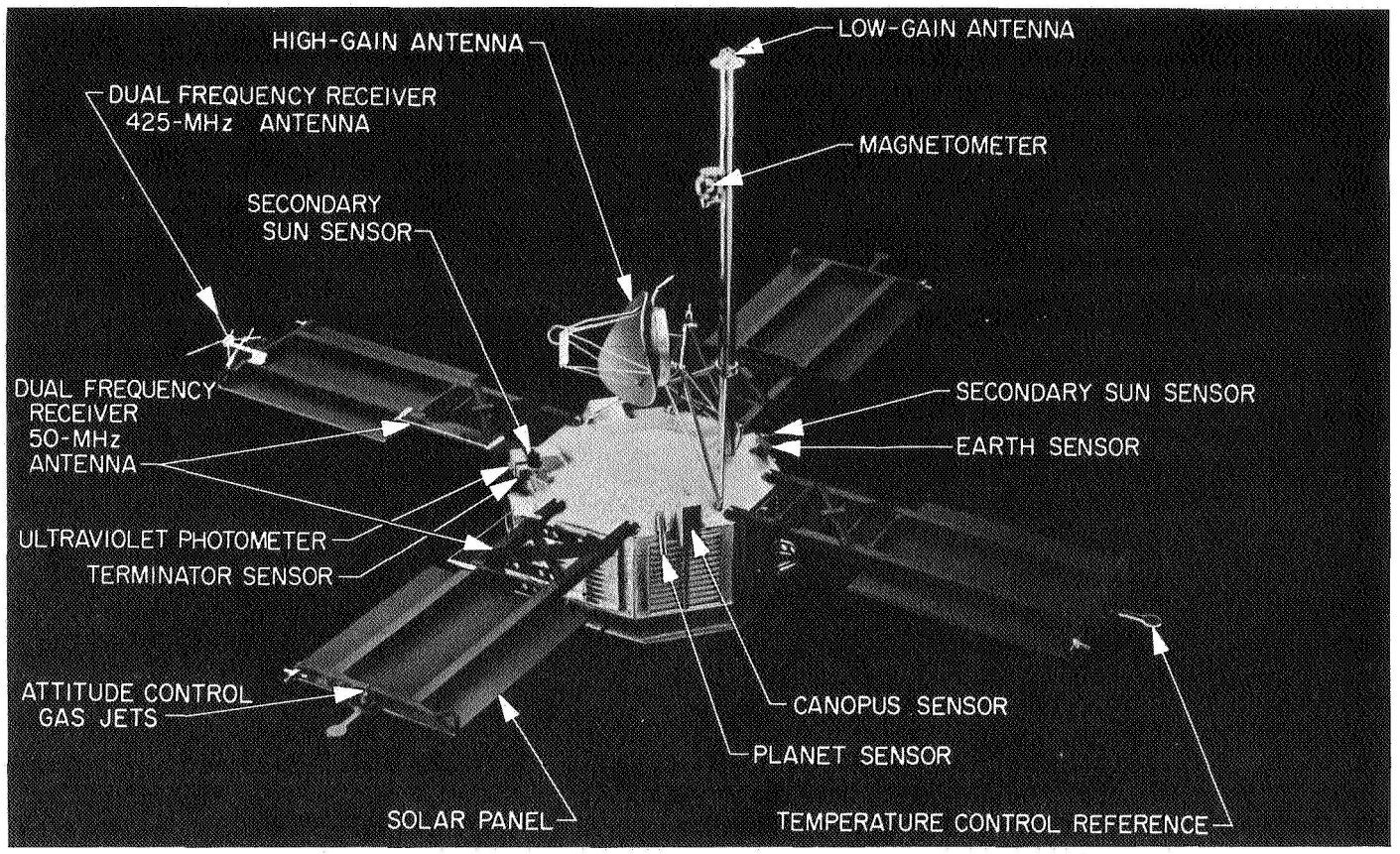

Fig. 2. *Mariner* Venus 67

View of side of spacecraft directed away from sun. Panel at lower left attached at Bay 1 with remaining panels attached at Bays 3, 5, and 7, proceeding clockwise

microscopic inspection, shortly before shipment to Cape Kennedy.

Special precautions were taken to guard against several sources of potential magnetic contamination to ensure that the spacecraft remained essentially demagnetized up to the time of launch. First, close surveillance of the demagnetized hardware was maintained so that, if the hardware were removed from the spacecraft assembly area, it could be rechecked and redemagnetized if necessary. Second, tools used in the assembly of the spacecraft were examined, and, where necessary, demagnetized to prevent inducing perm fields in the spacecraft. Third, the *Agena* adapter, shroud, and matchmate tools were monitored for magnetic fields and demagnetized as required.

Solar panels, which had been of major concern in the *Mariner* Mars program, were to be handled in the same manner in this program. Because the Venus mission necessitated a redesign of the solar panels, tests were made to determine whether demagnetization of the panel would be as effective as it had been for the earlier program. It was found that the redesign had magnetically improved the panel so that it would not acquire a residual field from the vibration testing. In fact, it was quite difficult to induce a measurable field in the panel. When the flight panels were mapped, it was likewise found that these panels had a negligible field and did not require demagnetization.

B. Control Plan

The following items were the main features of the magnetic control plan as it was actually carried out for *Mariner* Venus 67:

(1) ECRs were reviewed and discussions were held with cognizant engineers of hardware on which the magnetic quality might be affected by the

change. For questionable items, the magnetic quality was checked.

(2) At least one prototype or TA model of all flight hardware was subjected to an extensive magnetic evaluation involving:

(a) An initial "as received" mapping.

(b) A demagnetization in three orthogonal axes at a 1/20-Hz alternating frequency with a decreasing magnetic field having an initial peak value of 40 G.[1] This demagnetization was followed by a second mapping.

(c) The hardware was next exposed to a peak magnetic field of 25 G in the axis having the highest field component in the initial mapping. A third mapping was made following this exposure. In a few cases, the hardware was re-exposed in a different axis and re-mapped.

(d) Next, the hardware was demagnetized as in 2(b), but with an initial peak magnetic field of 80 G. A fourth magnetic mapping was then obtained.

(e) Finally, an attempt was made to determine the effect of an inducing field of approximately 0.25 G in each of the three coordinate axes. Interpretation of these results was not entirely satisfactory.

(3) All flight approval hardware for the spacecraft was demagnetized in three orthogonal axes with a 1/20-Hz decreasing alternating field having a peak initial value of 40 G and was followed by a magnetic mapping. This demagnetization and mapping was performed at the subassembly or, insofar as possible, at the assembly level during disassembly of the spacecraft for final inspection, after all vibration and shock testing of the hardware.

(4) Any hardware that was removed from the Spacecraft Assembly Facility (SAF) subsequent to the demagnetization in item (3) was remapped upon return to SAF and subjected to redemagnetization and remapping if the magnetic field had changed by more than 10% or 1 γ, whichever was greater.

(5) A TA solar panel was mapped, permed, and demagnetized several times with up to a 20-G 60-Hz demagnetizing field. All flight solar panels were magnetically mapped and found to have such low fields as to not require demagnetization.

(6) A single flight solar panel was examined for magnetic fields due to the flow of current in the panel.

(7) All tools used on the flight spacecraft or on matchmate in the SAF or at the Explosive Safe Facility (ESF) were examined for magnetic fields and demagnetized if the field on the surface of the tool exceeded 5 G. Periodic rechecking of the tools was also made.

(8) The *Agena* adapter and shroud were examined for magnetic fields and subjected to spot demagnetization as necessary.

This plan was implemented in March 1966 and a magnetic mapping, magnetization, and demagnetization facility was erected in the SAF building with testing of TA hardware being accomplished from June 1966 through February 1967. Demagnetization and mapping of flight hardware began in February 1967 with magnetic cognizance of the hardware maintained in varying degree until launch of the flight spacecraft on June 14, 1967.

III. Magnetic Test Facilities

Upon approval of the Magnetic Control Plan, it was necessary to establish facilities for performing the tests prescribed by the plan. To avoid the complications of mapping flight hardware that were encountered during the *Mariner* Mars 1964 program, because the mapping facility was accessible only by travel over several miles of road, the magnetic facility was located adjacent to the Spacecraft Assembly Area (SAA).

To satisfy the test requirements established by the plan, it was necessary that the facility be capable of magnetic mapping (magnetic field measurement) of hardware, magnetization of hardware by exposure to a fairly uniform magnetic field, and demagnetization of hardware by an alternating and decreasing magnetic field.

Results of the demagnetization tests on *Mariner* Mars 1964 PTM dictated that a low ambient field was necessary for effective demagnetization. Consequently, it was necessary to have a facility in which the effect of the earth's field on the hardware under test would be negligible.

For magnetization and demagnetization of the hardware, the pair of 7-ft-diam coils developed for the *Mariner*

[1]Throughout this report, the unit Gauss (G) is used in place of the more correct unit Oersteds (Oe) because of custom and because instruments used to measure these fields are calibrated in this unit. These units are approximately equivalent in air.

Mars 1964 program, to demagnetize the solar panels and the spacecraft bus structure, were used. These coils are described in Ref. 1.

While the Magnetic Control Plan required a facility at Cape Kennedy for continued monitoring and possible demagnetization of hardware, shipping costs and space limitations dictated a smaller and considerably lighter facility, for limited usage in mapping and demagnetizing flight hardware but not capable of TA demagnetizing field levels. As a consequence, two test facilities, one at JPL and a smaller one at Cape Kennedy, were utilized.

A. Magnetic Test Facility at JPL

The TA magnetic test specification[2] developed for this program established the following facility requirements:

(1) The magnetic test facility shall be located in the SAA.

(2) The facility will be capable of:
   (a) Reducing the earth's field magnitude to less than 250 γ over a spherical volume of at least 30 in. in diameter by means of an air coil system.

   (b) Generating a single-axis, constant-magnitude magnetic field of at least 25 G over a cylindrical volume of 6-ft length by 6-ft diam.

   (c) Generating a single axis 1/20 Hz alternating, pulsed demagnetized field of at least 80 G (57 G rms) over a cylindrical volume of 6-ft length and 6-ft diam and in the presence of the field requirement in item (a).

(3) The magnetizing and demagnetizing fields will be measured on the coil axis, midway between the two coils, with no test hardware in position. The desired field will be calibrated against coil current for subsequent adjustment of the field when the test hardware is in place. The demagnetizing and magnetizing fields will be continuously monitored, through a pickup loop, on a strip chart recorder.

The available area in the spacecraft assembly building was first surveyed with a rubidium total field magnetometer to determine the nature of the gradients in this steel frame building. After surveying the available area, a location in the area of minimum gradients was selected for erecting the magnetic mapping, magnetizing, and demagnetizing facility adjacent to the system test complex. The gradients in the center of the area in which the mapping would take place were on the order of 200 to 300 γ per ft.

As previously mentioned, two 7-ft-diam coils were used to generate the magnetizing and demagnetizing fields. These coils, placed coaxially with their axes approximately 7 ft above the floor and separated by 7 ft, were capable of producing a constant magnetic field on the axis, midway between the planes of the two coils, of 100 G. These coils were elevated to get further away from structural steel in the floor, with its higher gradients, and also to accommodate larger earth's field bucking coils.

For demagnetization of spacecraft flight hardware, the demagnetizing system was developed to generate a pulsed, alternating, and decreasing amplitude 1/20 Hz magnetic field that could not damage hardware by inducing damaging voltages in the circuitry. Because of the relatively large circuit inductance, analysis of the waveform of the demagnetizing field indicated that harmonics above 1 Hz were negligible. As with the constant field, the 1/20-Hz demagnetizing field also had a peak amplitude of 100 G. For 60-Hz demagnetization of solar panels, which was only performed on a TA panel, these coils were capable of approximately a 23-G rms field when tuned to series resonance.

To buck out the earth's field at the center of the demagnetizing coil system, large wood coil frames were fabricated and wound to form a three-axis Helmholtz coil system encompassing the demagnetizing coils. The largest Helmholtz pair, 12½ ft in diam, were used to cancel the vertical component of the earth's fields. Ten-ft diam coils, coaxial with the demagnetizing coils and oriented with their axes within a few degrees of magnetic East-West, were used to cancel the small variable East-West component of the earth's field. A pair of coils, 12-ft diam, were placed with their axes North-South to cancel this component of the ambient field. The arrangement of these coils is illustrated in Fig. 3.

After erection of this facility, and with the earth's field bucking coils energized and adjusted to reduce the ambient field to zero at the center of the approximately 2-ft[3] mapping area, the field gradients were again checked with a fluxgate gradiometer probe. Within a spherical volume of approximately 30 in. in diameter centered 1 ft above the center of the mapping turntable, the magnetic

[2]JPL Specification MVZ 50574-TAT, "Environmental Test Specification *Mariner* Venus 67 Flight Equipment Type Approval Magnetic Test Requirements (assembly and subassembly level)."

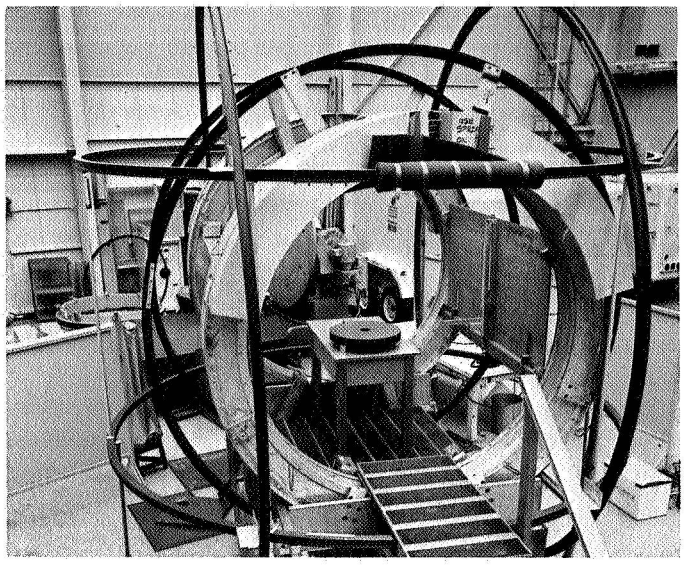

Fig. 3. Magnetizing and demagnetizing facility at Pasadena

field was less than 200 γ. During magnetic testing, the ambient field at the center of the coil system was not continuously maintained near zero, but was readjusted at least every three hours. It is estimated that most hardware was exposed to ambient fields of not more than 400 to 500 γ during either magnetic mapping or demagnetization.

With the coil system oriented with the earth's field, the large demagnetizing coils had a negligible effect on the bucking coil system. This was because of the small number of turns necessary on the East-West coil pair which were coaxial with the demagnetizing coils and would be most subject to demagnetizing transients.

To facilitate induced field measurements and to minimize the effect of the demagnetization on the magnetometer sensor, a fluxgate magnetometer probe was mounted on a bracket on the north side of the turntable with its axis North–South. The support and bracket were designed so that the mapping distance could be varied from 6 in. to 6 ft and the sensor could be raised or lowered, as necessary, so as to be directed at the approximate geometric center of the hardware to be mapped. The magnetometer probe was equipped with a compensating winding necessary for canceling the ambient field in the vicinity of the probe when it was moved further from the low field at the center of the coil system or when measuring induced fields in the presence of an ambient field.

As a result of the magnetization operation, the magnetometer sensor indicated a slight residual field apparently caused by the magnetization of components in the protective circuitry mounted on the demagnetizing coils. This condition had negligible effect on the post-perm mappings and was eliminated in the subsequent demagnetization operation.

Power for the three-axis, Helmholtz coil system was provided by two 36-V, 2-A, regulated, adjustable, constant voltage power supplies. A supply was used for the vertical field coils while the other furnished power to both the North–South and East–West coils. Provision was made for turning off the North–South coils, independent of the East–West coils, for furnishing an inducing field of approximately 0.25 G in the horizontal North–South axis. After an initial warmup, the bucking coils were adjusted at the beginning of each day of use and at least every three hours thereafter during the day. Adjustment consisted of reducing the ambient field, approximately 6 in. above the center of the mapping turntable, to approximately zero using the single-axis fluxgate magnetometer probe mounted in a rectangular plastic block. Each axis was individually adjusted and rechecked until it was within a few gamma of zero.

Power for the large demagnetizing coils was provided by two remotely programmable 36-V, 100-A power supplies connected in series through a polarity reversing relay to the series connected demagnetizing coils. These supplies were controlled by a programmer designed to furnish a 3-s voltage pulse of decreasing amplitude, every 10 s, which was caused to reverse polarity after each pulse by the polarity reversing relay. For the 25-G perm exposure operation, this same programmer was utilized, but with the decreasing amplitude feature disabled so that a constant amplitude but alternating pulse was obtained. Thus, the direction of final exposure could be controlled, and the hardware could be subjected to several reversals of perm. This was considered a more effective means of stabilizing the perm condition.

B. Magnetic Test Facility at Cape Kennedy

At Cape Kennedy, where only a 40-G demagnetization capability was required, and with no requirement for demagnetizing solar panels, a smaller and lighter weight facility was more practical. This facility consisted of a 10-ft-diam, 3-axis Helmholtz coil system with a 4½-ft-diam demagnetizing Helmholtz pair at the center. The demagnetizing coil axis was also aligned with the East–West field bucking coil axis to minimize interaction between the bucking and the demagnetizing coils.

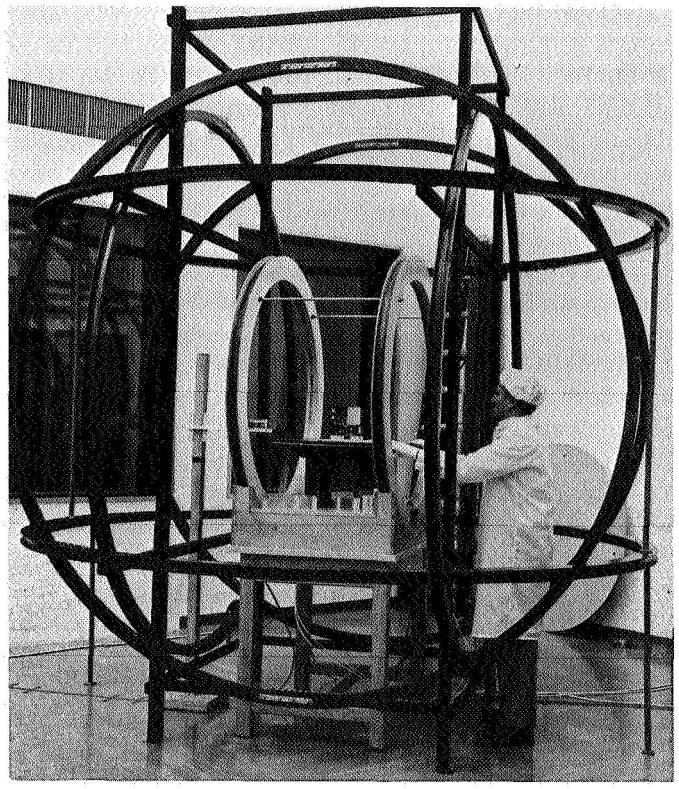

Fig. 4. Magnetic control test facility at Cape Kennedy

This facility was erected in a corner of the highbay of the Spacecraft Assembly Building, Hangar AO, at the Eastern Test Range at Cape Kennedy, adjacent to the two *Mariner* Venus 67 flight spacecraft. This facility is shown in Fig. 4.

Without the requirement for induced field measurements, and because of an interfering periodic magnetic field (believed to be caused by a nearby computer), the magnetometer probe had to be placed on the axis of the demagnetizing coils. This virtually eliminated the 1- to 2-γ, peak-to-peak, interfering signal.

IV. Magnetic Test Program

A. Test Philosophy

The magnetic test program was based on two premises: (1) the negligible opportunity to improve the spacecraft magnetic condition by material replacement or redesign, and (2) the magnetic condition of the spacecraft material is more stable in the least magnetized condition.

The major effort was to demagnetize (deperm) all spacecraft hardware at the latest possible time before launch to erase any previously acquired residual magnetization (perm). This perm is normally obtained incident to vibration testing on magnetic shakers. Except for solar panels, stray fields caused by current flow in circuits, or motion of magnetic materials and alternating or fluctuating fields, were not investigated or evaluated on the assembly or subassembly level in this program. Because of extensive redesign of the solar panels, current loop fields were redetermined.

This program did not have acceptance or rejection criteria for magnetics other than it be no worse than *Mariner* Mars 1964 hardware. Each item of hardware was subjected to a demagnetizing (deperming) field to reduce residual magnetization to the lowest possible value. There was an accept/reject criterion for safety to the spacecraft hardware; TA hardware was exposed to twice the amount (two separate operations) and twice the level of demagnetizing field (higher field) as the flight hardware. This verified that the operation was safe, and the mappings furnished information on the relative magnetic condition of the individual assemblies, the effectiveness of the demagnetization, and some measure of the magnetic stability to be expected.

Only the Canopus sensor (7CS8) was adversely affected by demagnetization. Because of magnetic material in the sensor, it was found that demagnetization altered the sensor alignment. As realignment necessitated partial disassembly of the sensor, a waiver of the demagnetization requirement was given in this case.

B. Type Approval Testing

To qualify the demagnetization process for the flight hardware, one nonflight (TA or prototype) model of the hardware was required to be magnetically evaluated and demagnetized to ensure that the demagnetization was effective and had no adverse effect on the operation or performance of the hardware.

The magnetic evaluation of spacecraft hardware consisted of measuring the radial component of the residual magnetic field of the test hardware at a fixed distance in each of three orthogonal planes through the approximate geometric center of the object after various magnetic treatments (magnetization and demagnetization) of the test unit. This measurement process is known as magnetic mapping of the hardware.

Each item of this type hardware was subjected to the following sequence of operations:

(1) Initial "as received" mapping.

(2) Demagnetization with initial peak field of 40 G.

(3) Remapping.

(4) Magnetization by exposure to peak field of 25 G.

(5) Remapping.

(6) Redemagnetization with initial peak field of 80 G.

(7) Remapping.

(8) Remapping for induced field effect.

Upon receiving hardware for test, it was initially determined if there were any restrictions on placing the hardware on the mapping turntable with mapping coordinates parallel to the spacecraft coordinates of the hardware. In cases where the hardware could not be placed on a side, because of protrusions or structural weaknesses, a different coordinate system was selected and related to the spacecraft coordinates. In a few cases, it was impossible to map the hardware in more than two of its three orthogonal planes; however, this was sufficient to determine the dipole moment. Each mapping orientation was photographed to ensure consistency in the numerous mappings of similar hardware and to facilitate analysis of the mapping data.

With the Helmholtz coil system adjusted to provide a near-zero magnetic field at the center of the system, the hardware to be tested was placed at the center of the mapping turntable with the $+x$ axis directed vertically upward, and the $+y$ axis directed at the magnetometer sensor. This position was identified as the x position. The magnetometer probe was positioned vertically to the approximate center of the hardware and placed at a distance from the center of the hardware of at least three times the maximum rectilinear dimension of the hardware. The actual measurement distance was selected from the following to satisfy the above requirement, but not over 6 ft; 6, 12, or 18 in.; 2, 3, 4, 5, or 6 ft. The turntable was then rotated 360 deg while an x-y plot was obtained of the radial magnetic field component versus the angle of rotation of the turntable. This plot then gave the radial component of the magnetic field in the y-z plane of the hardware at a fixed distance. The hardware was then rotated 90 deg about two axes to the following y position with the $+y$ axis vertically up, and the $+z$ axis pointed at the magnetometer probe. By rotating the turntable, a second plot was obtained for the radial field in the x-z plane. The hardware was again rotated about two axes to place the $+z$ axis vertical, and direct the $+x$ axis toward the magnetometer probe for the z position. The final rotation of the turntable resulted in the radial field plot in the x-y plane.

Because the area where these mappings were performed was sometimes noisy, several plots were obtained for the same position. Possible disturbances in the external ambient field could be detected by observing anomalies in the plot, or by comparing the field at the beginning and at the end of the rotation. The field closure in the 360-deg rotation was required to be less than 1 γ. At times, construction work in the area made it necessary to suspend testing or to perform the mappings in the evening when there was less external disturbance. Approximately midway through the program, it became standard practice to obtain several plots for each position, regardless of external disturbances, for comparison purposes, to reduce errors and improve the quality of the data. One source of error was caused by time lag in the rotation coordinate; repeated plots with opposite directions of rotation improved the determination of the angular position of the peak field.

In addition to the curves, recorded on the x-y recorder grid paper, information regarding the measurement distance, magnetometer scale multiplier, date, hardware identification, and type of test was recorded on the plot. Each plotted curve was identified with the axis of rotation of the hardware on the turntable. The type of test referred to the nature of the preceding magnetic treatment of the hardware, which served as the basis for the mapping.

The initial mapping of the hardware was to provide some measure of comparison between the magnetic mapping results performed on *Mariner* Mars 1964 hardware and the mappings performed on *Mariner* Venus hardware. Although the majority of the 1964 mappings had been performed following vibration testing, much of the 1967 TA hardware that was removed from the *Mariner* 1964 PTM had been demagnetized in the interim, during the demagnetization tests on the PTM. Consequently, this first mapping was of no real value except to establish an orientation for subsequent tests and, in some cases, highlight the magnetic fields acquired by the hardware either during the vibration tests or in the laboratories.

Experience gained in the *Mariner* Mars PTM demagnetization tests indicated that it would be preferable to demagnetize the hardware so that the largest component of the residual perm field would be attacked first. The "as received" mappings then served to identify the perm component that should be demagnetized first.

Following the "as received" mapping, the hardware was demagnetized at the same level and in the same manner as flight hardware would later be demagnetized.

The demagnetization was performed successively in each of the three coordinate axes, commencing with the axis most nearly parallel to the axis of the "as received" dipole moment. The 40-G deperm was selected to precede the 80-G deperm so that this 40-G deperm would be as similar to the flight hardware demagnetization as possible. This would not be the case if the 40-G deperm did not directly follow the "as received" mapping.

Demagnetization was accomplished by a 1/20-Hz, alternating, and decreasing pulsed magnetic field. The peak demagnetizing field magnitude decayed as shown in Fig. 5 for the 40- and 80-G deperms.

The 80-G deperm was similar to the 40-G deperm except for the higher initial field and the longer time to decay. The basis for both the 80- and 40-G initial peak demagnetizing field levels was primarily that the *Mariner* 1964 PTM had been tested at these levels with satisfactory results. Also, it was desired not to exceed the 95- to 100-G peak capability of the large demagnetizing coils. A further restraint was the JPL environmental test philosophy whereby the TA demagnetization level should be twice that of the flight hardware demagnetization.

Magnetization or perm of the hardware was performed to gain knowledge of the relative amount of magnetic material in the hardware and whether this material was magnetically soft or hard. By comparing this condition of the hardware with its demagnetized condition, as revealed by the two mappings, these two factors were qualitatively determined as well as providing a measure

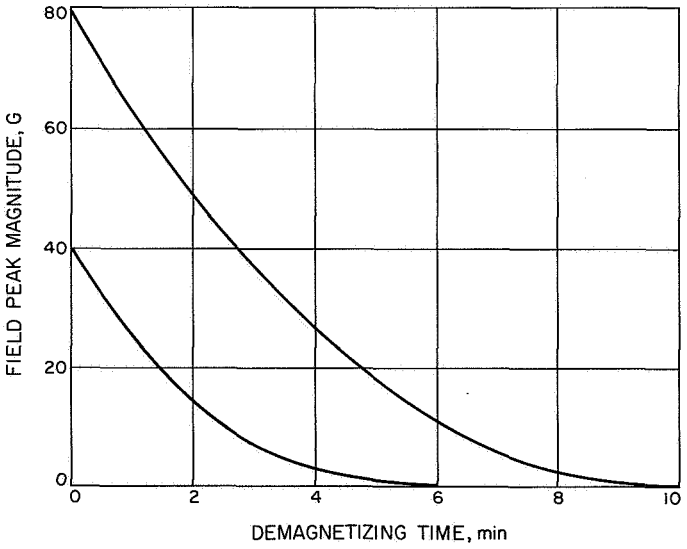

Fig. 5. Demagnetizing field decay curves

of the magnetic stability of the hardware exposed to external environments. To magnetize the hardware, it was exposed to a 25-G magnetic field. The magnetizing field was applied parallel to the axis most nearly parallel to the dipole observed in the "as received" mapping, or parallel to the axis which was believed to result in the largest perm. In general, time did not permit magnetizing in more than one axis, although this would have been desirable.

In retrospect, it would probably have been more beneficial, where time for only one perm exposure was available, to have exposed all hardware in either the positive or negative spacecraft z axis. Magnetization and demagnetization tests on *Mariner* 1964 PTM had indicated that the perm in this axis, on exposure, was approximately twice that obtainable in the x-y plane. Also, if the hardware had been permed in the x-y plane, the placement of the hardware on the spacecraft would have caused the x-y plane components to cancel out so that the net effect would be very low. On the other hand, a perm in the z axis would have resulted in a large field component and would have permitted a better comparison between the results of summing individually mapped subassembly fields and the measured field of the spacecraft.

The magnetizing field was produced in the same manner as the demagnetizing field except that, in this operation, the magnetic field was not permitted to decrease. Because it was desired to magnetize the hardware in the opposite direction from its normal perm dipole, the alternating pulsed field could be discontinued with the final pulse in either desired direction. The magnetizing field was then generated by a 1/20 Hz alternating, constant amplitude, pulsed field which was turned off after approximately 5 half-cycles in the desired direction so as to reverse the perm of the hardware. This permitted qualitative analysis of the hard perm component of the residual field. The low ambient field was unimportant for this operation, but was maintained for continuity and simplicity.

The induced field mapping was performed after the 80-G demagnetization so that the residual perm field would be as low as possible. The North–South axis, Helmholtz coil pair was turned off, resulting in a horizontal component of the earth's field of approximately 0.25 G in the axis of the magnetometer probe. The hardware was then mapped as described above for the perm field mapping except that, at the conclusion of a rotation of the turntable in which a suitable plot was obtained that was free of external disturbances, the hardware was removed from the turntable, and the turntable turned a

few degrees to mark on the plot the zero reference level for the ambient field. The hardware was mapped in each of its three rectilinear coordinates in this manner.

Only a cursory analysis was made of the induced field effect because of difficulty in interpreting the plotted data. This was because many of the items of hardware had an induced field that was a function of the relative direction of the inducing field. To analyze the induced field of these items would have initially required subtraction of the perm field component from the total measured field and a detailed analysis of the type, configuration, or amount of magnetic material in the various assemblies or subassemblies, both of which would have required considerably more time than was available. The induced field was not considered of major concern in this program.

The TA test program commenced on June 16, 1966 with tests on an attitude control gas system mounted on the structural test model of the bus structure. Because of the welded connections in the gas system, it was necessary to test the system as a complete assembly. Although the spacecraft has two independent systems for redundancy, only one of the two systems was tested. This system was subjected to the required magnetization and demagnetization operations in the x-y plane only; however, because of its size, it was impossible to properly map this structure without the spacecraft mapping fixture that was not available at the time. Unsuccessful attempts were made to determine the approximate field of the assembly by rotating the structure in the low field coil system while the bus structure was suspended from an overhead crane with the magnetometer placed at several different heights opposite the structure. Because demagnetization tests on the attitude control gas system components in the *Mariner* Mars program had indicated demagnetization was effective, it was not considered essential to obtain this mapping. It was subsequently verified that there was no adverse effect on this system performance caused by these magnetization and demagnetization operations.

The remaining TA magnetic tests were performed normally without difficulty. The results of spacecraft hardware mappings for major assemblies and subassemblies, except induced field mappings, are listed in the Appendix. For comparison, the results of the flight hardware mappings are listed with the TA test results. Several weeks following the magnetic testing of TA hardware, the cognizant engineer was contacted to determine whether there had been any effect on the operational performance of the hardware as a result of magnetic testing. All cognizant engineers, except the Canopus sensor cognizant engineer, reported no adverse effect on the hardware as a result of the TA magnetic tests.

C. Flight Hardware Demagnetization

Flight hardware was demagnetized during the disassembly of the two flight spacecraft for final microscopic inspection prior to reassembly, a brief system test, and shipment to Cape Kennedy. In the case of the spare flight spacecraft (MV67-1), this inspection was performed approximately two months prior to shipment to Cape Kennedy, with the spacecraft being essentially in storage during the intervening period. Disassembly of MV67-1 began February 9, 1967, and the spacecraft was demagnetized, mapped, inspected, and reassembled by February 15, 1967, at which time the assembled spacecraft was mapped on a large mapping fixture in the earth's field.

Insofar as possible, flight hardware was demagnetized and mapped in the same configuration as the TA hardware, except that flight hardware generally included harnesses that were not installed on the TA hardware. If the TA hardware was tested as a completed bay, so was the flight hardware; similarly, as in the case of the Science Bay, individual subassemblies were tested in each case. In a few cases, hardware was tested at both the subassembly and assembly levels.

Flight hardware demagnetization consisted of demagnetizing the hardware in three axes with a 40-G peak initial field decreasing and alternating at 1/20 Hz. Following demagnetization, the hardware was mapped in three axes and returned to the spacecraft area for inspection and reassembly.

Some cable harnesses and mechanical items of hardware that were expected to be free of magnetic material were waved a few inches in front of the magnetometer probe to verify that they were not magnetic.

In mapping the gyro subassembly (7A2) flight units, because of the extreme concern regarding damaging of the units by large angular accelerations, rotation of the hardware on the mapping turntable was restricted to 6 deg per second. This slow rotation made it difficult to obtain a mapping free of external disturbances. Intermittent disturbances during the course of the mappings necessitated a considerable amount of waiting for noise-free periods. With this and repeated rotations of the turntable sufficiently satisfactory data to permit proper analysis was obtained.

The TA magnetometer sensor (33A1), although necessarily nonmagnetic, apparently had sufficient magnetic contamination so that the sensor offset was affected by demagnetization. To stabilize this offset, each of the sensors was demagnetized prior to calibration of the instrument although the flight sensors did not exhibit this condition. The effect of the demagnetization was not detectable in the normal magnetic mapping of the instrument at a distance of 18 in.

The spacecraft was disassembled to the point at which the basic octagon, superstructure, attitude-control gas systems, the low-gain antenna, and some sensors, soldered into the wiring harnesses, were all that remained. This composite assembly, which was too large to map or demagnetize in the same manner as the smaller hardware, was demagnetized only in the spacecraft's x and y axes, while the assembly was suspended between the two large demagnetizing coils from an overhead crane. The assembly was then mounted on the large spacecraft mapping fixture and mapped in the earth's field in the same manner as the assembled spacecraft.

The MV67-1, after being in virtual storage for approximately six weeks, was remapped on March 31, 1967. It was found that there had been a material change in the mapped field as indicated in Table 1. This large change suggested that magnetic control efforts on this spacecraft had not been effective. In an attempt to investigate the cause of the large change in the spacecraft mapped field, the more magnetic items of spacecraft hardware were remapped, and, where a large change in field warranted, redemagnetized and remapped. A comparison of the summed field of these items of hardware at the time of the two mappings of the spacecraft accounted for about two-thirds of the change in the mapped field. During the period between the two spacecraft mappings, approximately three-fourths of the spacecraft hardware had been removed from the spacecraft assembly area and had been reworked in various laboratories or shops without subsequent verification of its magnetic condition. The following specific changes were made in the hardware of MV67-1 during the period:

(1) Subassembly 4A18 in Bay 1 was removed for rework.

(2) Midcourse motor was removed from SAF for rework and torque check of jet vane actuators was performed in high bay.

(3) Bay 3 was disassembled and all subassemblies were removed from SAF for rework.

(4) Bay 4 data encoder and command subassemblies were removed from SAF for rework.

(5) (a) Bay 5 tape recorder subassemblies were not demagnetized or installed in the spacecraft during the first spacecraft mapping.

(b) Bay 5 radio was reworked in SAF with undemagnetized tools.

(6) Bay 6 was reworked in SAF with undemagnetized tools, except 2RE1, 2PS2, and 2PS3 subassemblies which were removed from SAF for rework.

(7) The 7A1 subassembly was removed from SAF for rework.

(8) All louvers were removed from SAF for polishing.

(9) The trapped radiation detector was sent to the University of Iowa.

(10) The ultraviolet photometer was sent to the University of Colorado.

(11) The magnetometer was removed from SAF for rework.

(12) Canopus sensor S/N 001 was installed for the first spacecraft mapping while Canopus sensor S/N 107 was installed for the second mapping.

(13) The high-gain antenna was removed from SAF for rework.

Table 1. MV67-1 perm field mappings

Mapping date	Component of spacecraft field at spacecraft magnetometer position		
	P_x, γ	P_y, γ	P_z, γ
February 15, 1967	1.5	3.9	3.1
March 31, 1967	−1.0	3.3	6.9

After discovery of this weakness in the magnetic control plan, the plan was more strictly enforced so that this situation did not recur. The control plan had required that all hardware brought into the spacecraft assembly area after the initial demagnetization of the flight spacecraft be subject to a remapping and, if the maximum field extrapolated to 3 ft had changed by more than 10% or 1 γ, whichever was larger, the hardware was to be redemagnetized. This provision was to prevent the above situation from occurring and to keep hardware that was removed from the spacecraft for rework from being

reinstalled without a remapping verifying that no significant change had occurred in the hardware field. This procedure was faithfully followed for the remainder of the program, continuing at Cape Kennedy up to the time of launch of *Mariner V*. At ETR, between April 28 and June 13, 1967, 27 items of hardware required remapping and 6 items required demagnetization. The results of these mappings, as well as all other mappings of spacecraft hardware, have been listed in the Appendix by assembly or subassembly for both flight acceptance and TA tests. Only major assemblies and subassemblies have been included with this report; the data on the remaining items of hardware are available from the author.

The MV67-2 that was launched June 14, 1967, was disassembled for inspection, demagnetizing, and mapping between April 6 and 12, 1967. On April 13, the assembled spacecraft, less a subassembly in Bay 5 (2TR1), and the high-gain antenna was mapped as a unit. The results of this mapping were similar to the second mapping of MV67-1 (Table 2). The antenna had been mapped earlier and found nonmagnetic. Bay 5, with the missing subassembly reinstalled, was remapped and redemagnetized on April 15, 1967. The results of the various mappings of the assemblies and subassemblies of the two flight spacecraft are shown in Table 3.

D. Solar Panel Testing

Solar panels on the *Mariner* Mars 1964, before demagnetization, accounted for approximately three-fourths of the total spacecraft magnetic field. At the magnetometer, it was estimated that this field in the spacecraft z axis would be approximately 100 γ. Consequently, it was decided to demagnetize the solar panels with a 60-Hz demagnetizing field. The results were very satisfactory; the field of each panel was reduced to less than 1 γ at the sensor position.

For the *Mariner* Venus program, the solar panels were to be modified considerably to accommodate the flight toward, rather than away from, the sun, but would still be constructed with Kovar interconnecting bus strips and wires. The panel, as finally designed, had approximately two-thirds the active area of the earlier panels with the active surface on the opposite side and on the section of panel farther from the end which hinged to the spacecraft. This resulted in less Kovar on the panel (the offending magnetic material) and located it farther from the spacecraft magnetometer sensor.

The panel was electrically separated into three parallel sections to improve reliability and to minimize magnetic

Table 2. Final mapping of assembled MV 67 spacecraft (less solar panels)

Spacecraft	Field component at spacecraft magnetometer		
	x, γ	y, γ	z, γ
MV67-1 (March 31, 1967)	−1.0	3.3	6.9
MV67-2 (April 13, 1967)	−1.0	2.6	7.1

fields caused by current flow in the panel. With this arrangement, the Kovar bus strips and wires connecting the solar cells in series and parallel were oriented with their long axes across the width of the panel, rather than in the long axis of the panel, as was the case with *Mariner* 1964. In this orientation, the buses and wires were essentially at right angles to the shaker field and, consequently, did not acquire a magnetization from the shakers during vibration testing.

Early in the program, a study was made on the effectiveness of magnetization and demagnetization of a small section of a panel. This included a comparison of the effectiveness of 60 Hz versus 1/20 Hz demagnetization. The study revealed that the Kovar wires and strips could not be demagnetized with the available 60-Hz field normal to the axis of the buses, nor was 1/20 Hz pulse demagnetization in the axis parallel to the buses as effective as the 60-Hz field. Based on the results of this study, the facility used for demagnetization of *Mariner* 1964 panels was modified to accommodate the solar panel with its long axis at right angles to the axis of the coils and changed over for 60-Hz operation. A specification[3] was prepared on the magnetic test requirements for both TA and flight approval (FA) panels. The FA requirements were also included in a system level procedure[4], because, at the time of the test, the panels were under the control of the system test engineer.

A TA solar panel was then tested to determine the nature of its magnetic field and whether it could be effectively demagnetized in the modified facility. This panel (S/N 002), was first mapped in the earth's field in

[3]JPL Specification MVP-50661-ETS "Environmental Test Specification *Mariner* Venus 67 Flight Equipment, General Requirements for Magnetic Testing and Demagnetization of Type Approval and Flight Acceptance Solar Panels," November 30, 1966.

[4]JPL Procedure MV67 105.01 "*Mariner* Venus 67 Spacecraft Subassembly Demagnetization and Magnetic Mapping," March 21, 1967.

Table 3. Comparison of assembly and subassembly mapping results

Hardware nomenclature	MV67-1 February 13, 1967				MV67-1 April 3, 1967				MV67-2 April 12, 1967			
	Maximum radial field at 3 ft, γ	B_x, γ	B_y, γ	B_z, γ	Maximum radial field at 3 ft, γ	B_x, γ	B_y, γ	B_z, γ	Maximum radial field at 3 ft, γ	B_x, γ	B_y, γ	B_z, γ
Bay 1, power	15.8	−0.72	−0.54	−0.33	16.2	−0.91	−0.42	−0.31	14.4	−0.86	−0.44	−0.22
8A1/2 pyrotechnic control	11.5	−0.72	0	−0.48					10.4	−1.07	0.09	−0.07
8A1/2 pyrotechnic control	10.7	1.01	0.18	0.09					10.9	0.28	0.34	0.59
Bay 2, PIP	21.4	−0.98	−0.98	1.48	28.8	−1.65	−0.95	1.97	18.2	−0.88	−1.63	0.28
Bay 3 (includes following sub-assemblies)					4.3	−0.19	0.09	0.20	0.6	0.01	0.02	0.02
20A1-9 data automation system	1.2	−0.01	−0.05	0.07					1.4	0.04	−0.08	0.07
32A2 }	0.9	−0.08	0.01	0.01					0.3	0	0.02	−0.01
32A3 } plasma probe	0.2	0	−0.01	0.01					0.4	0	0.03	−0.01
32A4 }	0.4	−0.01	−0.02	0.02					0.1	0	0	0
33A2 }	0.3	−0.01	−0.01	0.03					0.6	−0.02	0.06	0.03
33A3 } magnetometer	1.1	−0.04	−0.06	0.08					0.6	0.04	−0.06	0.03
34A2 ultraviolet	0.3	0.01	−0.03	0.01					0.4	−0.03	0.01	0.02
35A1/2 DFR	0.5	0.01	0.03	0.01					0.4	0.01	−0.01	−0.01
DFR filters	4.9	0.67	−0.04	−0.09					1.0	0.11	−0.07	0.03
Bay 4, data encoder and command	16.0	1.43	0.33	−0.58	15.1	1.44	0.04	−0.43	11.7	1.29	0.42	−0.08
Bay 5, radio	4.0	0.47	0.09	0.05								
radio/tape	16.2	−1.76	−0.70	−0.40	19.6	−2.23	−0.99	0.02	24.3	−2.84	−1.69	−0.54
Bay 6, transponder	14.5	−0.96	0.69	0.76	14.6	−1.18	0.64	0.68	22.0	0.56	−2.41	0.66
Bay 7, central computer and sequencer	78.9	−0.05	9.71	2.57	85.8	0.84	10.50	2.78	86.4	1.50	10.41	2.93
7A2 gyro	1.1	−0.03	0.08	0.06	0.8	−0.05	−0.06	0.01	0.9	−0.05	0.04	0.04
Bay 8(4A8), power regulator	3.0	0.22	−0.10	0.19					3.8	0.22	−0.33	−0.16
4A14 battery	0	0	0	0					0	0	0	0
7CS8 Canopus sensor	23.7	0.96	−2.15	−2.71	21.0	1.52	−2.38	−2.31	14.3	1.58	−1.59	−1.44
25A1 TRD	0.4	0.03	−0.03	0.04					0.3	0.04	0	0.02
32A1 plasma probe	0.3	−0.02	−0.01	0.01					0	0	0	0
32A1 ultraviolet photometer	0.5	0	−0.06	0.03					0.3	0	0.02	0.01
S/C Bus w/gas system		−0.23	0.56	1.16						0.38	0.13	3.63
Bay 1, louver	0.3	0	0.01	0.01					0.4	0	0.01	0.02
Bay 3, louver	0.5	0.04	−0.01	0.02					0.5	0.01	−0.01	0.03
Bay 5, louver	0.6	0.04	0.07	0					0.5	0.02	0.03	0.03
Bay 6, louver	0.4	−0.05	0	−0.01					0.4	0.01	−0.02	−0.02
Bay 7, louver	0.1	0.01	0.01	0.01					0.2	−0.02	−0.01	−0.01
Bay 8, louver	0.3	−0.02	−0.01	0.02					0.3	0.01	0.02	0.02

a manner similar to that in which the spacecraft was mapped and as described in Ref. 2. Because the initial field was negligible, the panel was demagnetized with an initial field of 10 G rms in the presence of several permanent magnets from 3 to 6 in. from the surface of the panel and with their axes aligned with the long axis of the Kovar. The subsequent mapping disclosed a negligible change in the field of the panel. The panel was then demagnetized with an initial field of 10 G with similar results. The panel was again magnetized by demagnetizing in the presence of these permanent magnets, from 2 to 4 in. from the panel. This time, the panel had acquired a field of 6 γ in the axis parallel to the Kovar buses, across the width of the panel. The panel was then effectively demagnetized with an initial magnetic field of 20 G rms.

Based on these results, it was concluded that the magnetic field of the FA solar panels would be so low at the magnetometer as to be unmeasurable and, therefore, would not require demagnetization. This was verified with the mapping of each of the FA panels after completion of all environmental vibration and shock testing. The results of mapping of the FA solar panels are presented in Table 4; however, measurements are only accurate to approximately $\pm 0.3\ \gamma$.

Because of the complete electrical redesign of the *Mariner* Venus solar panel, it was considered necessary to determine the nature of the current loop (stray) magnetic fields at the position of the spacecraft magnetometer during interplanetary cruise conditions. The purpose of this test was to furnish the magnetometer experiment cognizant scientist with the expected effect of solar panel current flow on the magnetometer experiment. Because of the possibility that a portion of the panel may be damaged in flight, it was also desirable to know the field created by each of the three individually connected electrical sections of the panel. A structure was constructed to support a solar panel so that it could be oriented to face the sun and allow sufficient space behind and below the panel so that a three-axis magnetometer sensor could be placed at least 3 ft above the ground and in the same relative position to the panel as the flight magnetometer bears to the spacecraft solar panel in flight. This fixture is illustrated in Fig. 6. A spare flight solar panel (S/N 003), was tested on March 24, 1967 for these current loop-field components.

Table 4. Solar panel perm field mapping results

Solar panel and location on spacecraft	Magnetic field components at spacecraft magnetometer, γ		
	B_x	B_y	B_z
S/N 003 (spare) (+x)	0	0.1	0.1
(−x)	0.2	−0.1	0.2
S/N 004 (spare) (+x)	0	−0.1	−0.1
(−x)	0	0	0
S/N 005 (4A5)	0	−0.1	0
S/N 006 (4A7)	−0.3	0	0
S/N 007 (4A1)	0.2	0.2	0.2
S/N 008 (4A3)	−0.1	0	0
Total field S/N 005 through 008	−0.2	+0.2	+0.2

The solar panel is separated into three similar electrical sections across the width of the panel with each section having a clockwise current flow as viewed from the cell side of the panel. The field of each section, as well as the field of the whole panel, was measured for a panel in each of the four possible positions on the spacecraft. The values for each panel section, for each of the four spacecraft solar panel positions, are presented in Table 5. With the $+x$ and $+y$ panels and also the $-x$ and $-y$ panels being symmetrically located about the sensor, the positive axis panels should have similar values with the x and y components interchanged. The negative axis panels should likewise have similar values. With these measurements only accurate to $\pm$ ½ γ, it was considered desirable to average and extrapolate the measured results

Table 5. Solar panel current loop fields[a]

Solar panel position on spacecraft	Solar panel section A			Solar panel section B			Solar panel section C		
	x, γ	y, γ	z, γ	x, γ	y, γ	z, γ	x, γ	y, γ	z, γ
Bay 1 4A1 $+x$	−1.1	0.3	0	−1.7	0.2	−0.4	−0.9	0	0
Bay 4 4A3 $+y$	0	−0.9	−0.2	−0.3	−1.7	−0.6	0	−0.9	−0.2
Bay 5 4A5 $-x$	1.5	0	−0.4	2.4	−0.7	−1.0	1.3	−0.5	0
Bay 7 4A7 $-y$	0	1.8	0	0	2.3	−1.1	0	1.4	−0.5

[a]Field components in spacecraft coordinates in gamma for 600mA current per panel section.

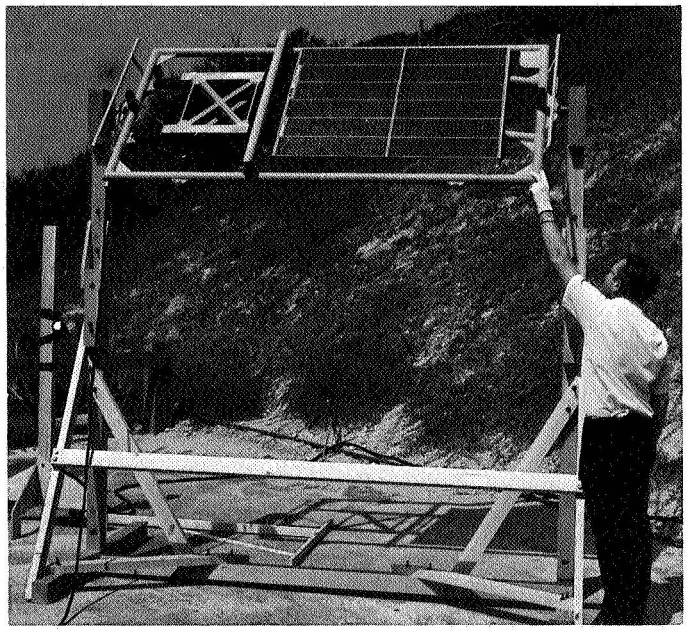

Fig. 6. Solar panel current loop testing

that were slightly different because of differences in the full load current. These corrected values are presented in Table 6.

In performing the current loop tests, it was necessary to shield the magnetometer probe to reduce the ambient field drift due to heating of the sensor by the sunlight.

E. Supplemental Studies

In addition to the regular test program, special tests were conducted in a few cases where particular concern was expressed by the hardware cognizant engineer about the demagnetization of his hardware.

With the decision that assemblies and subassemblies would be demagnetized, concern was expressed about the effect of demagnetization on permanent magnets

Table 6. Solar panel current loop tests

Test condition, solar panel S/N 003	Stray field component at spacecraft magnetometer location, γ		
	x	y	z
Panel in $+x$ position 1.8 A	−3.1	0	−0.7
Panel in $-x$ position 1.8 A	+5.2	−0.1	−1.7
Four panels on spacecraft cruise load 228 W	+1.5	+1.3	−3.4

which are a part of the latching relays employed in the central computer and sequencer (CC&S) as well as other units. The CC&S alone employs approximately 25 of these relays. This study was conducted to verify that demagnetization would not have an adverse effect on the relays.

Relays were tested by determining the maximum radial magnetic field at 8 in. and by measuring the minimum current required to cause a switching of the relay. These tests were made on a number of Sigma Type 32 and 33 relays and on the Potter and Brumfield SLG11D relay, following exposure of the relays to various peak demagnetizing field levels. The initial demagnetization of a latching relay appears to stabilize the relay magnetic field. This effect is independent of the demagnetizing field up to several hundred gauss. This initial stabilization results in a decrease of a few percent in the magnetic field. After this initial effect, the relay magnetic field is relatively unaffected up to a magnetic field of approximately 500 G peak. Beyond this field level, the residual external field of the relay rapidly decreases and the relay fails to latch after demagnetizing field levels of approximately 600 G peak.

When the ceramic, permanent magnet element of a relay was subjected to a demagnetizing field by itself, the maximum residual external field decreased by approximately 35% after a 100-G rms demagnetizing field. Because the magnet element consists of two opposing coaxial dipoles, this measured decrease may be a change in relationship of the two individual dipoles. It indicates, however, that the magnet receives considerable protection in the assembled condition where the magnetic circuit is more complete.

Tests of the current necessary to cause tripping of the relay showed considerably more variation between similar relays than was evident because of demagnetization, below approximately 500 G peak. Individual tripping or latching currents varied by as much as 15% from the mean tripping current, while deviation caused by demagnetization was less than 10% up to 565-G peak demagnetizing fields.

Essentially these same results were obtained by Goddard Space Flight Center in a similar, earlier test. These tests also alleviated concern felt by other engineers cognizant of such devices as motors and positioners, which have permanent magnet components.

The Canopus sensor, in addition to having ferromagnetic materials in the image tube, had a high-permeability

shield material around the tube to protect the tube electron beam from external stray fields that might affect the sensor's accuracy. Demagnetization of the complete sensor altered the alignment of this tube by approximately 0.5 deg, which was considered excessive. Because the sensor required disassembly to correct this alignment error, the flight Canopus sensors were granted a waiver on the demagnetization requirements.

Concern was expressed about the effect of demagnetization on the tape recorder tape. Tests on a specially prepared tape revealed that the magnetization and demagnetization of the tape recorder subassembly had no effect on the test recording on the tape because of the low fields employed in the magnetic control program.

F. Magnetic Mapping Data Analysis

One of the current means of evaluating the magnetic condition of spacecraft hardware components, subassemblies, and assemblies is to rotate the hardware about rectangular coordinates while recording the radial component of the magnetic field. Rotation about any two rectangular coordinates is sufficient to enable determination of the dipole moment of the hardware if the magnetic moment can be considered that of a simple dipole. The majority of spacecraft hardware satisfies this requirement if the mapping distance is at least three times the longest dimension of the hardware.

By mapping in each of the three orthogonal planes, and using just the amplitude of each of the three curves, the maximum radial component of the magnetic field of the hardware can be determined by the following equation (Ref. 3):

$$B_{max} = \left(\sum_{i=1}^{3} 1/8 \, B_i^2 \right)^{1/2}$$

where

B_i is the peak-to-peak amplitude of the curve obtained when the hardware is rotated about each of its rectangular coordinates (i=1,2,3).

This method was used in determining the magnetic condition of *Mariner* Mars 1964 hardware (Ref. 4).

The magnetic dipole moment, M, can be computed by the relation

$$M = 8.194 \, B_{max} \, d^3 \times 10^{-5}$$

where

M is in CGS units or G-cm^3; B_{max} is in γ; and d is the mapping distance in in.

In the *Mariner* Venus 67 program, it was desired to relate the magnetic mapping to the spacecraft coordinates of the hardware as mounted on the spacecraft structure and also obtain an extrapolation of the magnetic field to the position of the spacecraft science magnetometer sensor mounted on the spacecraft low-gain antenna. To accomplish the necessary computations in a reasonable time, a computer program was developed for use on an IBM 1620 computer which was readily available for use on short notice. The program that was finally developed was capable of determining the magnitude and orientation of the dipole moment in spherical coordinates directly related to the spacecraft rectangular coordinate system; the maximum radial component of the magnetic field at the measurement distance and also at a fixed distance of 3 ft; and the spacecraft x, y, and z components of the field at the spacecraft magnetometer sensor position.

The raw mapping data that were obtained from the x-y recorder consisted of three plots of the radial magnetic field versus the rotation angle as the hardware was rotated about each of its three rectangular coordinates. The particular rectangular coordinates used were selected to be either parallel to the spacecraft coordinate axes or easily converted to spacecraft coordinates by rotation about not more than two of the three axes. Where possible, these rotations of the mapping axis were directly related to spacecraft clock and cone angles.

From the x-y plot, the peak-to-peak amplitude of each of the three curves and the angular position of the positive and negative peak of each curve was obtained. The two angular positions were averaged to give positive and negative peak positions which were 180 deg apart. As one of the three plots provided redundant information, the two curves having the greatest peak-to-peak amplitude were used in the basic calculation with the peak-to-peak amplitude of the third curve providing a check on the maximum radial field as determined from the two curves alone. This check served as an indication of the dipole nature of the mapping.

The reason for averaging the angular position of the positive and negative peak of the curve was both because of the potential error in determining the peak of the curve and also because offsets of the dipole from the center of rotation caused the positive and negative peaks

to differ by other than 180 deg which is virtually corrected by the averaging technique. This method then results in a value for the positive peak which is more representative of the centered dipole and, therefore, is used in the subsequent computations. Tests on quadrupoles have also indicated that if the most positive and negative peaks are also averaged, where more than one positive and negative peak is obtained, better results are obtained.

In addition to the information obtained from the *x-y* plot, the mapping distance, the occasion for the mapping (previous magnetic history), the location of the center of gravity of the hardware in spacecraft coordinates, the coordinate rotations necessary to make the hardware coordinate axes parellel to the spacecraft axes, and the hardware and test identifications are included on the data card.

V. Magnetic Control of Spacecraft Integration

In addition to some spacecraft hardware being magnetic, there was the problem that magnetized material, not part of the spacecraft, would come into contact with the spacecraft and remagnetize it after it had been demagnetized. To preclude this possibility, several steps were taken:

(1) Requirements were imposed on the spacecraft launch vehicle to ensure that the spacecraft would not be magnetically contaminated from this source.

(2) Spacecraft assembly tools were monitored, and demagnetized (if required), to ensure that magnetized tools did not come in contact with demagnetized magnetic materials on the spacecraft.

(3) Metal fasteners (nuts, bolts, washers, etc.), when received for spacecraft assembly stock, were monitored to ensure that magnetic fasteners had not been mixed with nonmagnetic fasteners.

A. Spacecraft—*Agena* Interface

Magnetic requirements and constraints on the *Agena* vehicle, spacecraft adapter, and shroud were contained in the launch vehicle system requirements and restraints document, ED 348. This document required a knowledge of the magnetic fields of matchmate tools and equipment and the *Agena* adapter forward of *Agena* Station 247. It specified that any tools, equipment, or flight hardware that would come within 6 in. of the spacecraft at any time would be measured for a magnetic field on the surface of the item. It was required that, if fields greater than 5 G were discovered, the item would require demagnetization. It was also required that, during the *Agena* systems test, time be made available for JPL to perform a magnetic survey of the spacecraft adapter, diaphragm, and the exterior of the *Agena* forward equipment rack.

Because Lockheed Missile and Space Center, the *Agena* contractor, did not have adequate facilities for making the magnetic field measurements or for performing the necessary demagnetization, Lewis Research Center requested that JPL perform these operations for Lockheed.

On February 23, 1967, a magnetic survey was made of the *Agena* forward equipment rack at the Lockheed facility in Sunnyvale, California, to determine whether the *Agena* vehicle produced magnetic fields in the vicinity of the spacecraft adapter that might cause magnetic contamination of the spacecraft. As far as was known, magnetic fields about an *Agena* vehicle had not been previously observed or determined.

The *Agena* vehicle used for launch of the *Mariner* Venus was probed to determine the extent of its external magnetic fields. The forward equipment rack was surveyed with both a dc and ac gaussmeter with the vehicle in its several modes of operation. The vehicle was generally quite nonmagnetic with only three components having any measurable dc field. Its structure and equipment are fabricated of basically nonmagnetic materials with nonmagnetic fasteners apparently used throughout.

The power distribution box had a small area in the center of the face of the box, approximately in the plane of the spacecraft adapter (Station 247), in which the maximum measured field was 10 G. This field was attributed to latching relays within the box. On the end of the FM telemetry unit facing the spacecraft, a peak field of 20 G was detected. The source of this field was not definitely determined but was believed caused by a circulator. The third source was the C-band beacon adapter kit on which an 8-G field was measured. This latter unit is approximately 15 in. from the plane of the spacecraft adapter. In each of these areas, the field was quite concentrated and, therefore, was not considered a threat to the spacecraft.

In the various operating modes of the vehicle, no measurable fields were observed that could be attributed to the operating condition of the *Agena*, except for a 2-G field near the surface of the cables furnishing operational support equipment power at approximately 10 A to the vehicle. The only detectable ac field from dc through

30 kHz was approximately a 0.1-G, 400-Hz component in one area on the surface of the power inverter module.

On March 2, 1967, during matchmate tests of the shroud, spacecraft, and adapter at JPL, the shroud and adapter were surveyed with a gaussmeter for magnetic fields. The following items on the spacecraft adapter and shroud were magnetic and exceeded 5 G on the surface of the item:

(1) Approximately one-third of the bolts securing the adapter ring to the ground support equipment (GSE) ring (Station 247) exceeded 5 G.

(2) One of four spacecraft separation pistons had a field across the stem of the piston of 9 G.

(3) The large screw drive in the shroud spring cocking device exceeded 10 G and some of the screws holding the cocking devices to the shroud exceeded 5 G.

(4) The two pins in some shroud harness buckles exceeded 10 G.

Only the pushoff piston of item 2 was within 6 in. of the spacecraft and required demagnetization. These pistons and springs were rechecked on May 23, 1967 at Cape Kennedy on both the flight and standby spare adapters. Two pistons on one adapter and one on the other required demagnetization. The screws, item 1 above, were reported by a Lockheed engineer to be replaced by nonmagnetic screws when the adapter is mated to the *Agena* vehicle. As all other fasteners were nonmagnetic, this was not verified.

B. Assembly Tool Magnetic Control

Examination of tools used for spacecraft assembly and disassembly revealed magnetic fields as high as 140 G on the surface of the tool. More than 30 tools had fields greater than 50 G. Fields of this magnitude, while being quite concentrated, can cause measurable fields in spacecraft ferromagnetic materials if they come in contact with, or within a fraction of an inch of, the material. While the amount of this material on the spacecraft is small, such material is used throughout most of the electronic subassemblies and in some of the mechanical attachments, notably springs and spherical bearings. Because of the presence of this material, some precaution is necessary to ensure that magnetized tools and electrical meters do not induce perm fields in the spacecraft components after the spacecraft assemblies and subassemblies have been demagnetized.

Early tests were made on a small welded cordwood module to determine how much effect magnetized tools would have in inducing a perm field in the module. Unless the field on the surface of the tool exceeded 10 G, there was negligible perm field as a result of touching magnetized material on the surface of the module. It was also found that most tools, when properly oriented in the earth's field, have an induced field on their surface of as much as 2 to 3 G. Based on these results, it was decided that tools having a residual field on the surface in excess of 5 G would be considered a potential source of magnetic contamination and would be demagnetized to reduce the field below this level.

Initially, all spacecraft assembly tools were examined for a magnetic field by probing with a gaussmeter probe over the surface of the tool. Tools that were used for the assembly or disassembly of the spacecraft were kept in a large "rollaway" tool cabinet and tool box—one for each of the two spacecraft. These cabinets accompanied each respective spacecraft during all test operations. In general, these were the only tools used in working on the spacecraft. Where other tools were used, such as on the attitude control gas system, the midcourse propulsion system, or by Lockheed during matchmate of the spacecraft and *Agena* vehicle, these tools were also checked for magnetic fields prior to use on the demagnetized spacecraft.

The spacecraft assembly tools were first surveyed shortly before the spacecraft was disassembled for inspection and demagnetization. Other tools were examined at the time they were introduced into the spacecraft assembly area. Of approximately 1000 tools for each spacecraft, approximately one-third had fields greater than 5 G on the surface and were considered to have a residual magnetization.

All tools with a field exceeding 5 G were demagnetized with a decreasing 60-Hz magnetic field. Although the majority of tools were demagnetized with an initial field of 50-G rms, some tools required as much as 200-G rms to effectively demagnetize the tool.

Magnetization of the tools seemed to follow no pattern. Virtually every type of tool was magnetized from sockets and wrenches to screwdrivers and drill bits. In general, the long-pointed tools had the higher fields, with jeweler screwdrivers having quite high fields. Although it was expected that the field would generally be in the

long axis of the tool, many sockets had opposite poles on opposite sides of the socket and crescent wrenches had fields between the jaws of the crescent.

The two tool cabinets used with MV67-1 and MV67-2 were designated as G-5080 and G-5266, respectively. Tools in these two boxes, which were initially measured between January 19 and February 16, 1967 resulted in the distribution of measured fields shown in Table 7.

Table 7. Magnetic monitoring results

Spacecraft tool box	G-5080	G-5266
Approximate number of tools	1000	800
Number of tools with field $\geq$ 5 G	370	326
Number of tools with field $\geq$ 20 G	89	73
Number of tools with field $\geq$ 100 G	8	3

Each tool box was rechecked between April 14 and 17, 1967. Box G-5060 had 52 tools requiring redemagnetization, while Box G-5266 had 27 tools requiring redemagnetization. These boxes were again checked at the Air Force Eastern Test Range (AFETR) on May 5, 1967; approximately six tools in each box required redemagnetization.

Tools used by Lockheed in matchmate of the spacecraft adapter were monitored at the ESF at AFETR on May 25, 1967, immediately prior to matchmate. Approximately 25% of these tools required demagnetization to reduce their residual field to the acceptable level.

The cause of a subsequent perm field in tools, after the initial demagnetization, is not known. The tool boxes were checked and did not have a residual field and permanent magnets were excluded from the tool boxes. It is possible that the fields were acquired from the field of meters or permanent magnets in spacecraft components.

C. Magnetic Control of Fasteners

Spacecraft fasteners, notably screws, nuts, and washers, were checked to determine whether they possessed a field greater than 2 γ per lb when measured at 6 in. after exposure to a 100-G field. This requirement, which had been imposed on fasteners in the *Mariner* Mars program, was carried over in the requirements for stock fasteners in this program.

VI. Program Evaluation and Review

The magnetic control effort on this program had two major objectives: (1) to reduce the spacecraft magnetic field, and (2) to obtain a stable magnetic field at the science magnetometer sensor. Improvement was achieved primarily through demagnetization of the flight hardware. In addition, highly magnetic items of hardware used on the Mars spacecraft were deleted from the Venus spacecraft. This included the television system, the scan platform, and the ion chamber experiment. This last item had a noticeable effect on *Mariner* Mars because of its location within 2 ft of the magnetometer sensor. The data automation system, redesigned for the *Mariner* Venus 67 flight, was changed from cordwood module construction with its magnetic lead materials to less magnetic integrated circuits.

The second objective for obtaining a stable magnetic field was more difficult to verify. A comparison of the estimated magnetic field of the complete flight spacecraft and the magnetic field, as determined in space, shows a change in the spacecraft field. The MV67-2 was successfully launched from Cape Kennedy on June 14, 1967. While the spacecraft was rolling in space following sun acquisition, it was possible to determine the x and y components of the residual field of the spacecraft. It was also subsequently possible to statistically obtain a value for the z component of the field. These values are compared with the components of the total field of the spacecraft, including both spacecraft and solar panel perm and current loop fields for the particular operating condition of the spacecraft. This comparison is shown below:

Fields	x, γ	y, γ	z, γ
Field determined from current loop and perm mappings, April 13 to 15, 1967	−0.6	1.0	7.1
In-flight field determination, June 14 to 30, 1967	4.9	0.8	8.7

The differences between these values cannot be definitely explained, but are probably caused by the following:

(1) Several subassemblies were removed from the spacecraft for rework following the spacecraft mapping, with a consequent change in the subassembly field, although the hardware was remapped

and either displayed negligible change or was redemagnetized.

(2) Some subassemblies exhibited sufficient magnetic instability to be affected by the launch environment.

Additional factors bearing on this discrepancy are discussed in the following subsection.

A. Summation of Subassembly Fields

In addition to demagnetizing for a lower spacecraft field and for improving magnetic stability, it was also desired in this program to gain more knowledge on the magnetic characteristics of spacecraft hardware. Consequently, it was desired to determine whether the magnetic fields of spacecraft could be linearly combined to provide a satisfactory estimate of the total field of the assembled spacecraft. If this were the case, adding the field would be of considerable value in future magnetic control programs in following the reverse procedure of prescribing the permissible field of subassemblies on the basis of an overall system restraint. This is pertinent in any large program where the assembly and subassembly restraints must conform to and support the overall system requirements. In addition, it would be of advantage to predict the effect of removing or installing a single subassembly or assembly on the total spacecraft field.

To fulfill these goals, all hardware was mapped in a coordinate system that could be directly related to the spacecraft coordinates through a simple transformation. In most cases, this was directly in the spacecraft coordinates. If the hardware was restricted as to the sides on which it could rest during mapping, or if the hardware was installed on the spacecraft in an irregular manner, it was mapped in coordinates that would permit easy transformation. For most sensors, this was in terms of the cone and clock angles specified for the orientation of the hardware. It was primarily because of the necessity for these transformations in obtaining the field of the hardware in spacecraft coordinates that the data were computer processed. This processing also facilitated the summing of the magnetic field components of the hardware.

With a direct relation between the spacecraft coordinates and the coordinates in which the hardware was mapped, as well as a knowledge of the position of the spacecraft magnetometer and the position of the hardware on the spacecraft, it was relatively simple to determine the components of the magnetic field of the hardware at the position of the spacecraft magnetometer sensor. Computations, however, are completely dependent on the hardware behaving as a simple magnetic dipole in which the field can be easily extrapolated from one position to another. This assumption appears to be valid with approximately 90% of the hardware.

It is believed that mappings resulting in multipolar fields were one of the major sources of the differences between the summed and the mapped field. This was particularly evident in two different Bay 6 mappings in which, although the mapped curves were similar (both displayed a double-peak characteristic of a quadrupole and had approximately the same overall amplitudes), the positions of the higher peaks were such as to essentially indicate a reversed field at the magnetometer sensor. Whenever a multipolar mapping was obtained, attempts were made to improve the mapping by remapping at a greater distance up to the maximum distance of 6 ft. It was frequently found that an assembly or subassembly mapping resulted in a curve that was characteristic of a dipole not at the center of rotation. The effect of an offset dipole was assessed in Ref. 5. This information was of assistance in analyzing these magnetic mappings. When an offset dipole was apparent, the hardware was displaced on the turntable to bring the dipole source closer to the center of rotation, and the hardware was remapped. Thus, every effort was made to obtain a dipolar mapping so that the mapping information could be properly extrapolated to the magnetometer position.

In evaluating this technique of summing the magnetic field components, a comparison of the summed field was made with the field of the spacecraft as actually mapped in the earth's field a few days following the demagnetization and mapping of the individual units of spacecraft hardware. The spacecraft mapping, which is performed under the direction of the magnetometer experiment cognizant scientist as an aid to the analysis of the experimental data obtained in flight, is performed in the earth's field and is fully described in Ref. 5.

This mapping is made without solar panels; the solar panels are individually mapped. The results of the spacecraft and solar panel mappings are linearly combined, together with current loop-field determinations, to arrive at the total spacecraft field in flight under various cruise modes.

A comparison of the results obtained by adding the field components of individual assemblies and subassemblies with the measured field of the spacecraft obtained a few days later is shown in Table 8. The values given in Table 8 are for the assembled spacecraft, except that solar panels and their appendages are not mounted.

Table 8. Flight spacecraft summed and measured magnetic field components

Spacecraft and date of mapping	Type spacecraft field determination	Spacecraft field components at magnetometer (less solar panels)		
		x, γ	y, γ	z, γ
MV67-1, February 15, 1967	summed	0.9	7.4	2.2
	mapped	1.5	3.9	3.1
MV67-1, March 31, 1967	summed	−0.8	6.8	2.4
	mapped	−1.0	3.3	6.9
MV67-2, April 13, 1967	summed	−1.3	2.5	5.7
	mapped	−1.0	2.6	7.1

The attitude control gas system, however, is mounted on a much shorter dummy panel. The low-gain antenna and the spacecraft thermal shields and shades, which are completely nonmagnetic, are removed to facilitate the measurements and handling of the spacecraft.

Direct comparison of the three mappings (two spacecraft) should be weighed by the fact that there were some differences between the mapped configurations of the spacecraft. MV67-1 was mapped without the tape recorder subsystem and the gyro subassembly on both occasions while MV67-2 included these items, but was missing the high-gain antenna reflector and feed, which are nonmagnetic, and the Bay 6 transformer-rectifier, which is not. The summed fields, however, are for the same configuration in which the spacecraft was mapped.

In comparing the three mappings, it should be noted that the field of MV67-1 changed by as much as 4 γ between the two successive measurements taken approximately six weeks apart. This was not anticipated and it was partially on the basis that there would be a negligible change that the mapping of the spacecraft at Cape Kennedy was considered unnecessary and, therefore, not accomplished. Although a great deal of the hardware had been reworked during this period, this did not completely explain the large differences observed in the mappings.

The fact that there was a rather large change resulted in a remapping of the assemblies that had been removed from SAF for rework and had not been subsequently rechecked for magnetic changes. The spacecraft fields were again summed in an effort to explain the difference in the two spacecraft mappings. While the new summed field did show changes in the proper direction, the magnitudes of the y and z components still differed by some 3 γ each.

In comparing the summed field with the mapped field, a partial explanation can be made. There are three major difficulties associated with attempts to sum magnetic field components:

(1) Because of the generally random distribution and orientation of spacecraft magnetic field sources, it might be expected that, if they were approximately of the same magnitude, they would add algebraically to nearly zero. Consequently, only the unusually large sources, or nonuniform orientations or distributions, would be apparent.

(2) To extrapolate magnetic field data, it must be assumed that all sources can be represented by a simple dipole. This is not necessarily true for actual hardware. Although most hardware appeared to be a simple dipole at the measurement distance, a few exhibited multipolar characteristics. In general, this resulted in an extrapolated field component of less than normal magnitude. Similarly, if the mapping rotation is not about the dipole center, a greater than actual field magnitude is obtained.

(3) Subassembly magnetic fields are materially altered by even low concentration of ferromagnetic material in adjacent subassemblies. This apparently has the effect of shunting the subassembly field through the magnetic material so that the external fields of the assembly are reduced and modified.

It appears that, in general, the field of several assembled units will be less than the sum of the individually mapped subassemblies. This is supported by comparison of measurements made on completely assembled Bays 3 and 5 and the summed field of the equivalent individual subassemblies and subsystems making up these bays.

B. Analysis of Mapping Results

A review of the mapping results reveals that some units showed an excessively large variation in successive mappings of the same unit. This was particularly evident with the midcourse motor, the Canopus sensor, the gyro subassembly, the data encoder and command assembly (Bay 4), and the radio system (Bays 5 and 6). In each of these cases, there was more than a 20% variation between supposedly equivalent mappings of similar hardware. In the case of the midcourse motor, the gyro, the Canopus sensor, and Bay 6, which all have a great deal of magnetic material including some hard magnets, these

changes must be due to differences in the physical assembly of some parts which affect the air gaps involved.

As noted in the mapping results presented in the Appendix, there are approximately 12 assemblies that have a maximum field greater than 2 γ at 3 ft and, consequently, are the major contributors to the magnetic field at the science magnetometer sensor. Unfortunately, these assemblies include most of the above items, which in addition to displaying instability, map either as a multipole or off-center dipole. Of these, the central computer and sequencer, Bay 7, produces several times the field of any other unit and is the principal source of the spacecraft residual field. In attempting to explain differences between the summed and mapped fields, mapping errors were studied. The effect of both angular and magnitude errors in interpreting the Bay 7 data were analyzed because of the high field of this package. It was found that errors in the relatively high magnetic field assemblies could not have exceeded 10%.

Magnitude and angle were readable to better than 5%. These measurement errors cannot possibly account for the large discrepancy between summed and measured fields.

The results of the 40-G demagnetization of the TA and flight assemblies were quite similar in all cases except for the midcourse motor. In this case, the flight hardware had a magnetic field approximately four times that of the TA unit, and the dipole moment was approximately reversed in direction.

Multipolar fields were most evident in mappings of the radio system (Bays 5 and 6), the midcourse motor (Bay 2), and the ultraviolet photometer (34A1). The greatest difficulty in interpreting data, because of an apparent offset dipole, was with the data encoder and command system (Bay 4), the pyrotechnic control units (8A1/2), and the power system in Bay 1.

Investigation of the change in field caused by the attitude control jets being in flight configuration on the end of the solar panels, rather than on the dummy solar panel racks, indicated a negligible effect. Similarly, the change in field caused by the change in position of the high-gain antenna, produced by the antenna pointing change at encounter, had negligible effect on the spacecraft field.

In general, hardware, as received, had a relatively high residual field, in some cases even higher than that caused by the 25-G exposure field. In most cases, these fields could be effectively reduced by demagnetization. The results indicated that some assemblies, however, were not sufficiently demagnetized by the 40-G deperm level.

In a few cases, the field, after an 80-G demagnetization, was greater than the field determined in either the "as received" or 40-G deperm mappings. This apparently was caused by a permanent magnet part as well as other magnetic material in the hardware.

Magnetic stability of the hardware can best be inferred by comparing the 25-G exposure mapping and the 40-G deperm mapping as well as by comparing similar mappings of the same or different serial hardware. Large differences in both cases are indicative of potential instability in the magnetic field.

In demagnetizing the coax cables 2W2 and 2W45 made of RG142B/U and cable 2W47 made of RG188, an attempt was made to accomplish the demagnetization with a 60-Hz demagnetizer in the earth's field. These cables, which are quite magnetic, became much worse after the initial demagnetization. It was impossible to demagnetize them in the earth's field and the only way in which these cables could be satisfactorily demagnetized was by demagnetizing them in a low ambient field. A few other mechanical devices behaved in a similar manner.

C. Spacecraft Current Loop Fields

The determination of the spacecraft stray fields was under the direction of the magnetometer experiment cognizant scientists, again because of the importance of these data in interpreting flight data. The current loop fields, also commonly called stray fields, are those magnetic fields caused by the flow of current in the spacecraft circuitry during various modes of operation. Although both flight spacecraft were checked for current loop fields, minor differences in the test conditions necessitated using a weighted average of the two results.

Current loop tests were conducted in the late evening hours when external magnetic disturbances were at a minimum. Changes in the magnetic field at the spacecraft magnetometer sensor were monitored during the spacecraft system tests as changes in operational modes were made.

Results shown in Table 9 were obtained for the four normal operational modes. The values shown are for the magnetic field components in spacecraft coordinates at the spacecraft magnetometer sensor and do not include solar panel current loop fields.

Table 9. Spacecraft current loop fields

Fields	x, γ	y, γ	z, γ
Pre-Canopus acquisition (solar power)	−3.0	−0.7	+0.4
Cruise mode (solar power, gyros off)	−1.6	−1.4	+1.8
After switching to TWT amplifier	−1.1	−0.9	+2.2
Encounter mode	−0.6	−0.9	+1.9

Table 10. Changes in current loop fields

Fields	Δx, γ	Δy, γ	Δz, γ
Switch from solar to battery power	−1.2	+1.6	+1.6
Switch from cavity to TWT amplifier	+0.5	+0.3	+0.3
Switch from exciter A to B	−0.4	+0.7	+0.4
Switch battery charger to boost mode	−1.4	0	−0.3
Turn on gyros	−1.4	+0.7	−1.4

Current loop field changes associated with changes in operational modes that yielded measurable effects are given in Table 10.

VII. Conclusion

While redesign limitations have severely restricted any material improvement in the *Mariner* Venus 67 magnetic quality, the spacecraft magnetic field is lower and believed to be more stable than it would have been without these efforts. Without effort, the magnetic condition could very easily have become much worse. However, the magnetic stability of the spacecraft is very suspect. Magnetic stability remains intimately related to the amount and type of magnetic material in the hardware, while the total spacecraft field is more dependent on placement and orientation of hardware on the spacecraft.

This program was unable to strike at the heart of the magnetic control problem. The only available means of improving the magnetic stability of the spacecraft field was to minimize the use of soft magnetic materials. It is not enough to merely reduce the total field of the spacecraft or the field at the magnetometer sensor. The numerous dipole sources on the spacecraft have a natural tendency to cancel each other because of their random distribution and orientations. Consequently, a spacecraft with a low net magnetic moment or low field at its magnetometer sensor could very easily be made up of a large number of very magnetic assemblies or subassemblies. Physical separation is another technique that can be utilized to reduce the magnetic field at the magnetometer. If the more magnetic assemblies can be located further from the sensor than the less magnetic assemblies, or if the less stable assemblies are further away, the magnetic quality of the spacecraft is improved. In both cases, magnetic control must start very early in the conceptual design stages; much earlier than was possible in this program.

Magnetic mapping techniques can be improved to minimize errors and provide data in a more usable form, while the analysis of data should be developed to the point where results are not dependent on a simple dipole mapping. The technique of summing subassembly fields to arrive at an estimate of the total spacecraft field does not appear to be entirely valid in arriving at quantitative results because there is sufficient ferromagnetic material in adjacent assemblies to shunt and distort the field from that obtained for the subassembly alone. However, it appears that summing the fields gives a worst-case result which is still of value in analyzing the spacecraft fields and in providing insight into the qualitative effects.

Several theoretical questions have arisen in this program which could be the subject of further study:

(1) Why is 60-Hz demagnetization more effective than 1/20-Hz demagnetization?

(2) Can the magnetic quality of spacecraft hardware be predicted on the basis of its magnetic constituents and their characteristics?

(3) Can magnetic stability be quantitatively defined in a usable manner?

A study on effective shielding techniques for containing the field of permanent magnets would be of a more practical value. The assembly on this spacecraft that contributes the majority of the field, because of many latching relay magnets, might very easily be reduced to an acceptable level by shielding. Certainly the instability evident in the midcourse motor and the radio system should be more thoroughly investigated.

References

1. Frandsen, A. M. A., "Design of Spacecraft Degaussing Coils," in *Proceedings of the Magnetics Workshop, March 30–April 1, 1965.* Technical Memorandum 33-216, pp. 239–254, Jet Propulsion Laboratory, Pasadena, Calif., Sept. 15, 1965.
2. Bastow, J. G., "Solar Panel Deperming," in *Proceedings of the Magnetics Workshop, March 30–April 1, 1965.* Technical Memorandum 33-216, pp. 255–267, Jet Propulsion Laboratory, Pasadena, Calif., Sept. 15, 1965.
3. Frandsen, A. M. A., "Magnetic Mapping of *Mariner* Mars Assemblies," in *Proceedings of the Magnetics Workshop, March 30–April 1, 1965.* Technical Memorandum 33-216, pp. 197–204, Jet Propulsion Laboratory, Pasadena, Calif., Sept. 15, 1965.
4. Bastow, J. G., *Mariner Mars Spacecraft Magnetic Contamination Status Report.* Technical Memorandum 33-261, Jet Propulsion Laboratory, Pasadena, Calif., Feb. 1, 1966.
5. Lackey, M. H., Jr., *Magnetic Moment Testing of Satellites.* NOLTR 64-52, Naval Ordnance Laboratory, White Oak, Maryland, Jan. 18, 1965.
6. Stallkamp, J. A., "*Mariner* Mars Magnetic Mapping Tests," in *Proceedings of the Magnetics Workshop, March 30–April 1, 1965.* Technical Memorandum 33-216, pp. 107–124, Jet Propulsion Laboratory, Pasadena, Calif., Sept. 15, 1965.

Appendix

Mariner Venus 67 Magnetic Mapping Test Results

This appendix contains the results of magnetic mapping performed on *Mariner* Venus 67 hardware major assemblies and subassemblies. In Table A-1, assemblies or subassemblies listed give the test results for each mapping made on that item of hardware.

Type approval tests are listed ahead of the mappings performed on flight hardware. While the mappings of the flight hardware are in the sequence in which they were performed, the TA hardware is listed with the 40-G deperm mapping last, preceded by the 80-G deperm mapping to facilitate a comparison of these mappings after demagnetization, with the similar flight hardware mappings.

In Table A-1, information is listed for each of the eight spacecraft bays (not necessarily complete bays, as noted); the individual subassemblies that were not mapped as part of the assembled bay; and the major independently mounted scientific and guidance sensor assemblies. The electronic subassemblies for the scientific experiments were mapped both individually and as a part of the complete Bay 3, as indicated in the remarks column. The actual serial number, or the distinguishing identification of the particular item of hardware mapped, is given in the second column. The mapping basis in the third column identifies the nature of the immediately preceding treatment of the hardware which would alter or have an effect on the magnetic condition of the hardware.

PART A

FOLDOUT FRAME

Hardware nomenclature	Serial number	Mapping basis	M dipole moment, CGS	θ Angle from z axis, deg	ϕ Angle x-y pl from axis,
Bay 1, power (less 8A1/2)	02	As received	67.1	161	9(
	02	25-G perm	19.4	139	7
	02	25-G perm	102.5	174	(
	02	80-G deperm	55.1	173	33
	02	40-G deperm TA	56.3	170	3
	V16	40-G deperm FA	60.2	171	9
	V16	Reworked	61.8	167	7
	V16	40-G deperm FA	61.8	171	5
	V17	40-G deperm FA	55.4	163	6
	V17	Reworked	54.9	167	5
Bay 2, PIP (drawing 4700600)	MC-002	As received	28.2	96	21
	MC-002	25-G perm	57.8	93	22
	MC-002	80-G deperm	18.9	90	21
	MC-002	40-G deperm TA	21.9	99	21
	MC-006	40-G deperm FA	81.9	76	4
	MC-006	40-G deperm FA	88.0	81	4
	MC-006	Reworked	108.6	83	5
	MC-006	Reworked	103.2	83	4
	MC-006	40-G deperm FA	107.1	84	5
	MC-006	40-G deperm FA	110.3	76	3
	MV67-2	40-G deperm FA	99.1	107	6
	MV67-2	40-G deperm FA	108.8	114	7
	MV67-2	Reworked	91.7	137	9
	MV67-2	Reworked	74.8	125	9
	MV67-2	40-G deperm FA	89.6	138	9
	MV67-2	40-G deperm FA	69.7	142	7
Bay 3 (data automation system only, except as noted) (20A1-20A9)	073	As received	5.2	45	9
	073	25-G perm	150.8	93	17
	073	80-G deperm	0.8	67	7
	073	40-G deperm TA	2.7	60	7
	071	40-G deperm FA	4.7	64	7
	MV67-1	Reworked	16.4	42	3
	072	40-G deperm FA	5.4	72	9
	MV67-2	40-G deperm FA	2.3	15	9
Bay 4, data encoder and command	2/3	As received	196.7	93	15
	2/3	25-G perm	520.3	90	31
	2/3	80-G deperm	46.1	56	22
	2/3	40-G deperm TA	52.7	119	22
	201/V5/V6	40-G deperm FA	61.1	124	21
	201/V5/V6	Reworked	57.8	127	20
	401/V8	40-G deperm FA	44.8	99	20
Bay 5, radio receiver, tape	PTM	As received	89.3	82	13
	PTM	25-G perm	208.0	90	27
	PTM	25-G perm	384.9	81	18
	PTM	80-G deperm	39.4	70	7
	PTM	40-G deperm TA	40.2	68	8
	V7/V5	40-G deperm FA	15.3	109	19

FOLDOUT FRAME

FOLDOUT FRAME

PART B

FOLDOUT FRAME

Table A-1. *Mariner* Venus 67 assembly and subassembly magnetic mapping results

B_{max} at 3 ft, γ	Measurement distance, ft	B_{max} at measurement distance, γ	B_{max} from three measured amplitudes, γ	Components of magnetic field at spacecraft magnetometer sensor, γ			Total field magnitude at spacecraft sensor, γ	Distance from hardware CG to sensor, in.	Notes
				x	y	z			
17.5	4	7.4	7.3	−0.90	−0.86	−0.34	1.29	76	
5.1	4	2.1	2.3	−0.25	−0.39	−0.01	0.46	76	
26.8	4	11.3	10.8	−1.74	−0.39	−0.53	1.86	76	
14.4	4	6.1	6.1	−0.94	−0.13	−0.29	0.99	76	
14.7	4	6.2	6.1	−0.99	−0.36	−0.23	1.08	76	
15.8	4	6.6	6.5	−0.72	−0.54	−0.33	0.96	79	
16.2	4	6.8	6.9	−0.86	−0.55	−0.30	1.06	78	
16.2	4	6.8	6.9	−0.91	−0.42	−0.31	1.05	78	
14.5	4	6.1	6.2	−0.84	−0.55	−0.20	1.02	78	
14.4	4	6.1	6.1	−0.86	−0.44	−0.22	0.99	78	
7.4	4	3.1	3.2	0.47	0.29	−0.45	0.71	76	
15.1	3	15.1	15.5	0.83	0.82	−0.92	1.49	76	Quadrupole when perm reversed
5.0	3	5.0	5.2	0.36	0.20	−0.29	0.50	76	Offset in dipole in all measurements
5.7	3	5.7	6.0	0.33	0.24	−0.36	0.54	76	
21.4	6	2.7	2.6	−0.98	−0.98	1.48	2.03	75	
23.0	4	9.7	9.6	−1.17	−1.17	1.56	2.27	75	
28.4	4	12.0	11.6	−1.12	−1.82	1.89	2.85	75	
27.0	6	3.4	3.3	−1.36	−1.47	1.82	2.71	75	
28.0	4	11.8	12.3	−1.05	−1.86	1.85	2.83	75	
28.8	6	3.6	3.5	−1.65	−0.95	1.97	2.74	75	Offset in dipole, possible quadrupole
25.9	6	3.2	3.3	−0.86	−2.47	1.26	2.90	75	
28.5	4	12.0	11.4	−0.73	−2.91	1.14	3.21	75	
24.0	4	10.1	8.6	−0.52	−2.40	0.26	2.47	75	
19.6	6	2.4	2.5	−0.27	−2.08	0.43	2.14	75	
23.4	4	9.9	8.2	−0.48	−2.33	0.22	2.39	75	
18.2	6	2.3	2.3	−0.88	−1.63	0.28	1.87	75	
1.3	3	1.3	1.6	0.03	−0.02	0.07	0.08	78	
39.5	3	39.5	39.5	3.64	−0.69	−0.72	3.77	78	Offset dipole
0.2	3	0.2	0.6	0	−0.01	0.01	0.01	78	
0.7	3	0.7	0.7	0	−0.02	0.04	0.04	78	
1.2	3	1.2	1.1	−0.01	−0.05	0.07	0.09	78	Not simple dipole
4.3	4	1.8	1.4	−0.19	0.09	0.20	0.29	76	Complete Bay 3, not simple dipole
1.4	3	1.4	1.2	0.04	−0.08	0.07	0.11	79	Not simple dipole (20A1 S/N 73)
0.6	3	0.6	0.9	0.01	0.02	0.02	0.03	76	Complete Bay 3 with data automation system S/N 72 and all science
51.4	5	11.1	10.8	5.09	−2.30	1.94	5.91	74	Offset dipole
136.1	5	29.4	28.4	−11.10	8.44	−6.44	15.36	74	Slightly offset dipole
12.1	5	2.6	2.5	0.71	1.11	0	1.32	74	Offset dipole and slight quadrupole
13.8	5	3.0	2.9	1.06	0.60	−0.61	1.36	74	
16.0	5	3.5	2.8	1.43	0.33	−0.58	1.58	74	
15.1	5	3.3	2.9	1.44	0.04	−0.43	1.50	74	Offset dipole
11.7	5	2.5	2.5	1.29	0.42	−0.08	1.36	74	Offset dipole in y axis slight quadrupole
23.4	5	5.0	5.0	1.69	−1.80	1.03	2.68	73	
54.4	5	11.8	11.6	−0.12	6.38	−1.17	6.49	73	Perm in y axis Quadrupole in x-y plane
100.7	5	21.7	21.6	10.75	2.21	3.80	11.61	73	Perm in x axis Slight offset in dipole
10.3	5	2.2	2.4	−0.38	−1.06	0.30	1.17	73	Quadrupole
10.5	5	2.3	2.3	−0.34	−1.06	0.34	1.16	73	Quadrupole
4.0	4	1.7	1.7	0.47	0.09	0.05	0.48	73	Tape units not installed

FOLDOUT FRAME 2

FOLDOUT FRAME FOLDOUT FRAME

Table A-1. (contd)

Hardware nomenclature	Serial number	Mapping basis	M dipole moment, CGS	θ Angle from z axis, deg	ϕ Angle in x-y plane from x axis, deg	B_{max} at 3 ft, γ	Measurement distance, ft	B_{max} at measurement distance, γ	B_{max} from three measured amplitudes, γ	Com space
										x
Bay 5, radio receiver, tape (contd)	System 7/V1/V2	40-G deperm FA	58.3	96	19	15.2	4	6.4	6.6	−1.6
	System 7/V1/V2	40-G deprem FA	61.9	90	19	16.2	5	3.5	3.5	−1.7
	System 7/V1/V2	Reworked	138.3	77	6	36.2	4	15.3	14.0	−4.5
	System 7/V1/V2	40-G deperm FA	74.8	67	28	19.6	5	4.2	4.2	−2.2
	System 8/V2/V3	40-G deperm FA	95.7	87	27	25.0	4	10.6	10.4	−3.0
	System 8/V2/V3	40-G deperm FA	92.9	90	28	24.3	5	5.3	5.2	−2.8
	System 8/V2/V3	Reworked	82.8	80	28	21.7	4	9.1	8.9	−2.6
	System 8/V2/V3	Reworked	81.7	85	25	21.4	5	4.6	4.6	−2.6
	System 8/V2/V3	40-G deperm FA	75.3	81	27	19.7	4	8.3	8.0	−2.4
	System 8/V2/V3	40-G deperm FA	74.0	83	31	19.3	5	4.2	4.0	−2.2
Bay 6, radio xmtr.	3	As received	160.3	83	144	41.9	6	5.2	5.2	4.1
	3	As received	157.5	90	142	41.2	6	5.2	5.2	4.1
	3	25-G perm	972.4	81	138	254.4	6	31.8	31.9	22.8
	3	25-G perm	996.9	86	169	260.8	6	32.6	32.6	31.6
	3	25-G perm	1001.9	97	298	262.1	6	32.8	32.5	−15.2
	3	80-G deperm	41.5	26	168	10.9	6	1.4	1.3	0.4
	3	40-G deperm TA	45.9	90	141	12.0	6	1.5	1.7	1.1
	7	40-G deperm FA	55.4	37	308	14.5	5	3.1	3.1	−0.9
	7	Reworked	55.8	41	318	14.6	5	3.2	3.2	−1.1
	8	40-G deperm FA	88.0	52	112	23.0	5	5.0	4.7	0.6
	8	40-G deperm FA	84.2	51	111	22.0	6	2.8	2.6	0.5
	8	Reworked	97.0	51	124	25.4	6	3.2	2.8	1.1
Bay 7, central computer and sequencer (less gyro)	TA	As received	372.2	96	264	97.4	6	12.2	12.3	1.4
	TA	25-G perm	473.2	96	84	123.8	6	15.5	14.8	−2.3
	TA	80-G deperm	316.0	79	282	82.7	6	10.3	10.4	−1.4
	TA	40-G deperm TA	311.5	85	270	81.5	6	10.2	10.4	0.4
	006/004/005	40-G deperm FA	301.8	94	271	78.9	5	17.1	17.0	−0.0
	006/004/005	Reworked	318.7	89	264	83.4	5	18.0	17.9	1.4
	006/004/005	40-G deperm FA	327.8	93	267	85.8	5	18.5	18.3	0.8
	007/005/006	As received	799.3	87	273	209.1	5	45.2	45.1	−0.2
	007/005/006	As received	800.8	93	274	209.5	6	26.2	26.1	−1.4
	007/005/006	40-G deperm FA	338.1	94	271	88.4	5	19.1	18.5	−0.0
	007/005/006	40-G deperm FA	330.3	90	264	86.4	6	10.8	10.6	1.5
	007/004/005	Reworked	309.7	90	273	81.0	5	17.5	17.6	−0.1
	007/004/005	Reworked	305.9	91	273	80.0	6	10.0	10.0	−0.1
Bay 8, power (4A8)	02	As received	12.6	104	151	3.3	4	1.4	1.6	0.1
	02	25-G perm	31.8	86	321	8.3	4	3.5	3.5	−0.5
	02	80-G deperm	13.8	100	135	3.6	4	1.5	1.8	0.1
	02	40-G deperm TA	18.6	90	141	4.9	4	2.1	2.2	0.3

FOLDOUT FRAME FOLDOUT FRAME

FOLDOUT FRAME

nts of magnetic field at magnetometer sensor, γ		Total field magnitude at spacecraft sensor, γ	Distance from hardware CG to sensor, in.	Notes
y	z			
−0.68	−0.46	1.80	73	Radio system 8, tape system 7, with Louver 39. Quadrupole at 4 ft. Slight QP at 5-ft.
−0.70	−0.40	1.94	73	
−0.43	−0.73	4.63	71	Offset dipole in x-y plane, slight quadrupole in y-z plane
−0.99	0.02	2.44	71	
−1.63	−0.52	3.45	70	Slight offset in dipole } 2TRI not installed
−1.69	−0.54	3.35	70	
−1.37	−0.27	3.00	70	2TRI V6 installed
−1.29	−0.42	2.96	70	
−1.19	−0.27	2.72	70	
−1.38	−0.25	2.68	70	
−3.19	0.47	5.25	72	With accelerometer on handling frame
−3.18	0.13	5.20	72	Slight offset in dipole
−21.91	2.72	31.78	72	Perm parallel to face of panel in x-y plane
−6.63	4.70	32.64	72	Perm normal to face of panel
29.23	−0.23	32.97	72	Perm parallel to face of panel but 180 deg from above perm
−0.29	0.65	0.83	72	Slight offset in dipole
−0.96	0.03	1.51	72	
0.69	0.76	1.41	70	Strong quadrupole in all mapping planes with predominant field opposite to that of TA unit
0.64	0.68	1.50	70	
−2.51	0.69	2.68	70	Offset and slight quadrupole
−2.41	0.66	2.56	70	Offset and slight quadrupole
−2.48	0.91	2.89	70	Replacement relay installed at ETR
12.04	2.72	12.43	71	Dipole offset toward 7A1 unit for all TA mappings
−14.41	−4.82	15.38	71	
8.95	4.09	9.95	71	
9.56	3.31	10.13	71	
9.71	2.57	10.04	71	Slightly offset dipole
9.96	2.94	10.49	71	
10.50	2.78	10.89	71	Deperm y-axis only
24.72	8.41	26.11	71	
25.49	7.35	26.57	71	
10.87	2.90	11.25	71	
10.41	2.93	10.92	71	
9.74	3.03	10.20	71	Central computer and sequencer units from MV-1
9.70	2.88	10.12	71	
−0.13	−0.21	0.32	75	Not simple dipole
0.52	0.46	0.87	75	
−0.25	−0.20	0.37	75	
−0.31	−0.26	0.52	75	

FOLDOUT FRAME 12

PART A

FOLDOUT FRAME

Hardware nomenclature	Serial number	Mapping basis	M dipole moment, CGS	θ Angle from z axis, deg	Ang x-y p fro axis,
Bay 8, power (4A8) (contd)	06	40-G deperm FA	11.5	101	1
	03	40-G deperm FA	14.6	83	1
Gyro (7A2)	011	As received	3.2	104	4
	011	25-G perm	148.3	87	18
	011	80-G deperm	3.6	26	6
	011	80-G deperm	3.6	29	5
	011	40-G deperm TA	2.1	24	2
	011	40-G deperm TA	2.3	6	
	017	40-G deperm FA	3.1	67	4
	013	40-G deperm FA	4.4	69	29
	016	40-G deperm FA	3.4	70	31
	017	Reworked	12.7	102	30
	017	40-G deperm FA	1.3	30	
	016	Reworked	7.5	79	31
	016	40-G deperm FA	1.6	70	31
Tape recorder subsystem (16A1-6)	See note	As received	67.2	87	24
	See note	25-G perm	98.0	84	26
	See note	25-G perm	47.1	90	10
	See note	80-G deperm	33.5	90	21
	See note	40-G deperm	34.8	110	16
Canopus sensor (7CS8)	103	As received	68.1	69	13
	103	25-G perm	64.7	87	32
	103	80-G deperm	54.4	93	13
	103	40-G deperm TA	57.6	88	14
	103	As received	84.3	88	13
	103	25-G perm	56.9	84	31
	103	25-G perm	163.1	90	13
	103	25-G perm	62.8	108	13
	103	25-G perm	60.8	65	14
	103	80-G perm	71.4	47	14
	103	50-G perm	67.3	57	13
	103	80-G perm	134.5	86	31
	107	As received	82.5	81	13
	001	As received	90.5	108	13
	001	As received	90.8	108	13
	107	As received	80.2	91	13
	106	As received	54.6	74	13
	106	As received	68.5	112	13
	107	As received	75.7	9	13
	001	As received	73.0	104	13
	001	As received	71.9	101	13
	107	As received	77.5	90	13

FOLDOUT FRAME

FOLDOUT FRAME PART B FOLDOUT FRAME

Table A-1. (contd)

B_{max} at 3 ft, γ	Measurement distance, ft	B_{max} at measurement distance, γ	B_{max} from three measured amplitudes, γ	Components of magnetic field at spacecraft magnetometer sensor, γ			Total field magnitude at spacecraft sensor, γ	Distance from hardware CG to sensor, in.	Notes
				x	y	z			
3.0	4	1.3	1.7	0.22	−0.10	−0.19	0.31	75	
3.8	4	1.6	1.6	0.22	−0.33	−0.16	0.43	75	Slight offset dipole
0.8	1.5	6.7	5.3	−0.06	−0.05	−0.01	0.08	76	Quadrupole (x-y plane)
38.8	3	38.8	39.1	3.89	0.72	−0.69	4.02	76	
1.0	1.5	7.6	7.6	0	−0.06	0.03	0.07	76	
0.9	3	0.9	0.9	0	−0.06	0.03	0.07	76	
0.6	1.5	4.4	4.4	−0.01	−0.02	0.02	0.03	76	No adverse effect on torquer scale factor; IOM 344-795, R. Shrake to R. Crawford, 8/5/66
0.6	3	0.6	0.6	0.01	−0.02	0.03	0.04	76	
0.8	2	2.8	2.3	−0.05	−0.06	0.01	0.08	77	Quadrupole
1.1	2	3.9	3.9	−0.03	0.08	0.06	0.10	77	Not simple dipole
0.9	2	3.0	3.0	−0.05	0.04	0.04	0.08	77	
3.3	2	11.2	11.6	−0.21	0.26	0.09	0.35	77	Offset in dipole
0.3	2	1.2	1.2	−0.01	−0.01	0.02	0.02	77	Mapping rotation limited to 6deg per second
2.0	2	6.6	6.7	−0.12	0.12	0.09	0.19	77	Slight offset in dipole
0.4	2	1.4	1.5	−0.02	0.02	0.02	0.03	77	
17.6	4	7.4	3.4	0.83	2.01	−0.25	2.19	72	Multipolar fields: 16A1, S/N 2
25.6	4	10.8	11.1	0.22	3.12	−0.61	3.19	72	16A2, S/N 1
12.3	4	5.2	6.0	0.30	−1.40	0.48	1.51	72	16A3, S/N 3
8.8	4	3.7	4.6	0.90	0.62	0.11	1.10	72	16A4, S/N 3
9.1	4	3.8	4.0	1.04	−0.38	0.22	1.13	72	16A5, S/N 5
									16A6, Prototype
17.8	4	7.5	7.6	2.11	−2.01	−1.68	3.36	63	
16.9	5	3.7	3.5	−1.42	1.57	1.97	2.89	63	Slight offset in dipole
14.2	4	6.0	6.1	1.03	−1.54	−1.60	2.45	63	
15.1	4	6.4	6.5	1.43	−1.39	−1.73	2.64	63	
22.1	4	9.3	8.1	1.95	−2.31	−2.46	3.90	63	
14.9	4	6.3	6.2	−0.95	1.63	1.67	2.52	63	Perm in x axis
42.7	4	18.0	18.4	3.34	−4.72	−4.72	7.46	63	Permed in reverse direction
16.4	4	6.9	6.8	0.81	−1.32	−1.93	2.47	63	y-axis perm
15.9	4	6.7	6.8	2.06	−1.62	−1.48	3.01	63	Perm reversed
18.7	4	7.9	8.0	2.63	−1.89	−1.19	3.45	63	Special test y-axis perm
17.6	4	7.4	7.6	2.34	−1.90	−1.39	3.32	63	Special test 100-G deperm and reverse perm
35.2	4	14.8	14.7	−2.24	4.02	3.88	6.02	63	Special test x-axis perm after 60-G deperm
21.6	4	9.1	8.8	2.03	−2.51	−2.27	3.95	63	Less baffle
23.7	4	10.0	10.0	0.96	−2.15	−2.71	3.59	63	
23.7	3	23.7	23.6	0.97	−2.16	−2.72	36.1	63	
21.0	4	8.9	8.7	1.52	−2.38	−2.31	3.65	63	
14.3	4	6.0	6.3	1.58	−1.59	−1.44	2.66	63	
17.9	4	7.6	7.2	0.56	−1.52	−2.04	2.60	63	Excessively noisy mapping
19.8	4	8.4	8.4	1.55	−2.19	−2.19	3.46	63	
19.1	3	19.1	19.4	0.95	−1.84	−2.19	3.01	63	Offset dipole
18.8	4	7.9	8.2	1.01	−1.95	−2.13	3.06	63	Slight offset dipole
20.3	4	8.6	8.5	1.59	−2.24	−2.24	3.54	63	

FOLDOUT FRAME FOLDOUT FRAME 2

Table A-1. (contd)

Hardware nomenclature	Serial number	Mapping basis	M dipole moment, CGS	θ Angle from x axis, deg	ϕ Angle in x-y plane from x axis, deg	B_{max} at 3 ft, γ	Measurement distance, ft	B_{max} at measurement distance, γ	B_{max} from three measured amplitudes, γ	Con spac
										x
Magnetometer sensor (33A1)	Life test	As received	0	—	—	0	1.5	0	0	0
	0	40-G deperm FA	0	—	—	0	1.5	0	0	0
	1	40-G deperm FA	0	—	—	0	1.5	0	0	0
Magnetometer electronics (33A2)	Life test	As received	119.7	82	79	31.3	3	31.3	32.0	−0.5
	Life test	25-G perm	96.1	90	274	25.2	3	25.2	25.2	−0.3
	Life test	80-G deperm	1.7	126	4	0.4	1.5	3.5	3.4	−0.0
	Life test	40-G deperm TA	4.6	88	16	1.2	1.5	9.7	9.4	−0.1
	Life test	40-G deperm TA	4.0	72	105	1.1	3	1.1	1.3	0.0
	0	40-G deperm FA	2.8	61	67	0.7	2	2.5	2.2	−0.0
	5	40-G deperm FA	2.4	84	283	0.6	1.5	4.9	4.8	−0.0
	5	Reworked	2.9	86	319	0.8	1.5	6.1	5.9	−0.0
	5	Reworked	2.9	69	304	0.7	2	2.5	2.5	−0.0
	5	40-G deperm FA	2.4	85	285	0.6	1.5	5.1	4.9	−0.0
Magnetometer electronics (33A3)	Life test	As received	1.8	131	7	0.5	1.5	3.7	3.6	−0.0
	Life test	25-G perm	145.7	5	342	38.1	3	38.1	38.1	−0.0
	Life test	25-G perm	145.0	4	225	37.9	1.5	303.4	298.5	0.5
	Life test	80-G deperm	2.4	131	18	0.6	1.5	5.1	4.1	−0.0
	Life test	40-G deperm TA	1.8	111	13	0.5	1.5	3.8	3.6	−0.0
	1	40-G deperm FA	4.0	74	66	1.1	1.5	8.5	8.3	−0.0
	2	40-G deperm	2.1	97	129	0.6	1.5	4.4	4.4	0.0
	2	Reworked	2.3	102	121	0.6	1.5	4.9	4.8	0.0
	2	Reworked	2.3	83	112	0.6	1.5	4.9	4.6	0.0
UV photometer (34A1)	MC-3	As received	7.7	38	224	2.0	3	2.0	1.9	0.1
	MC-3	As received	10.7	42	215	2.8	1.5	22.3	17.6	0.2
	MC-3	25-G perm	50.1	83	45	13.1	3	13.1	12.9	−0.7
	MC-3	25-G perm	49.1	96	50	12.8	1.5	102.8	101.9	−0.7
	MC-3	80-G deperm	1.3	154	195	0.3	1.5	2.6	2.9	0
	MC-3	40-G deperm TA	1.7	107	65	0.4	1.5	3.5	3.8	−0.0
	MC-4	40-G deperm FA	1.9	134	95	0.5	1.5	4.0	4.1	0
	MC-4	Reworked	1.6	125	103	0.4	1.5	3.3	3.4	0.0
	2	40-G deperm FA	1.2	32	15	0.3	1.5	2.4	2.1	0
	2	Reworked	1.3	51	30	0.3	1.5	2.7	2.2	−0.0
UV photometer electronics (34A2)	MC-3	As received	8.6	48	91	2.3	1.5	18.1	17.6	0.0
	MC-3	25-G perm	14.6	83	277	3.8	1.5	30.5	32.5	−0.1
	MC-3	80-G deperm	0.6	57	42	0.2	1.5	1.3	1.1	−0.0
	MC-3	40-G deperm TA	2.3	47	36	0.6	1.5	4.8	4.4	−0.0
	4	40-G deperm FA	1.0	104	111	0.3	1.5	2.2	2.2	0.0
	MC-2	40-G deperm FA	1.4	58	15	0.4	1.5	3.0	3.1	−0.0
	MC-2	Reworked	1.7	52	28	0.4	1.5	3.5	3.5	−0.0
	MC-2	40-G deperm FA	1.2	57	30	0.3	1.5	2.5	2.8	−0.0
Dual frequency receiver (35A1/2)	1	As received	4.2	47	69	1.1	2	3.7	3.6	−0.0
	1	25-G perm	18.7	115	3	4.9	2	16.5	15.2	−0.4
	1	25-G perm	17.7	90	288	4.6	2	15.7	16.0	−0.1
	1	80-G deperm	0.6	38	195	0.1	2	0.5	0.4	0.0
	1	40-G deperm TA	1.7	21	255	0.4	2	1.5	1.3	0.0
	2	40-G deperm FA	2.0	171	141	0.5	1.5	4.2	4.0	0
	2	Reworked	1.9	162	180	0.5	1.5	3.9	3.9	0.0
	3	40-G deperm FA	1.4	155	203	0.4	1.5	3.0	3.0	0.0
	2	Reworked	2.0	180	—	0.5	1.5	4.2	3.9	0

nts of magnetic field at magnetometer sensor, γ		Total field magnitude at spacecraft sensor, γ	Distance from hardware CG to sensor, in.	Notes
y	z			
0	0	0	0	
0	0	0	0	
0	0	0	0	
−2.61	2.57	3.71	70	
2.44	−1.94	3.14	70	
−0.02	0	0.05	70	
−0.02	0.04	0.16	70	Quadrupole in x-z plane
−0.07	0.08	0.11	70	
−0.03	0.06	0.07	70	
0.06	−0.04	0.07	70	Offset in dipole
0.06	−0.03	0.10	70	
0.08	−0.03	0.10	70	
0.07	−0.04	0.08	70	
−0.02	0	0.05	72	
2.81	1.05	3.00	72	
2.86	0.93	3.06	72	
−0.04	0	0.07	72	
−0.02	0.01	0.05	72	
−0.06	0.08	0.11	72	
−0.05	0.03	0.07	72	Slight offset in dipole
−0.06	0.03	0.08	72	
−0.05	0.04	0.07	72	
0.18	−0.10	0.26	70	Slight quadrupole
0.22	−0.15	0.37	70	Strong quadrupole
−0.46	1.19	1.47	70	
−0.76	1.17	1.59	70	Offset in dipole
−0.02	−0.01	0.02	70	Not simple dipole
−0.04	0.04	0.06	70	Quadrupole
−0.06	0.03	0.07	70	
−0.05	0.02	0.05	70	
0.02	0.01	0.02	70	Quadrupole and offset
0.01	0.02	0.02	70	Quadrupole
−0.05	0.16	0.19	71	Offset in dipole for all TA mappings
0.40	−0.25	0.48	71	
0	0.01	0.01	71	
0.01	0.04	0.05	71	
−0.03	0.01	0.03	71	
0.01	0.02	0.04	71	Offset in dipole
0.01	0.03	0.04	71	
0	0.02	0.03	71	
−0.02	0.07	0.08	76	
−0.12	−0.01	0.49	76	Perm in x axis } slight offset in dipole
0.36	−0.24	0.46	76	Perm in y axis }
0.01	0	0.01	76	
0.04	0	0.04	76	
−0.03	−0.01	0.03	76	Offset in dipole
−0.03	−0.01	0.03	76	
−0.01	−0.01	0.02	76	Offset dipole in x-z plane
−0.03	−0.01	0.03	76	Excessively noisy mapping

Hardware nomenclature	Serial number	Mapping basis	M dipole moment, CGS	θ Angle from z axis, deg	Ang x-y fro axis
Pyro control (8A1/2)	1005	As received	41.6	7	3
	1006	As received	38.2	180	-
	1005	25-G perm	30.4	3	
	1006	25-G perm	30.1	174	3
	1005	80-G deperm	42.1	0	-
	1006	80-G deperm	40.9	178	
	1005	40-G deperm TA	42.2	0	-
	1006	40-G deperm TA	37.7	180	-
	1009	40-G deperm FA	44.0	170	2
	1010	40-G deperm FA	40.9	14	1
	1014	As received FA	42.1	26	
	1014	40-G deperm FA	41.5	26	
	1014	Reworked	40.7	22	
	1013	40-G deperm FA	40.3	157	
	1013	Reworked	39.8	162	3
Trapped radiation detector (25A1)	C101	As received	48.8	63	2
	C101	25-G perm	19.7	16	2
	C101	25-G perm	18.7	162	
	C101	80-G deperm	1.8	63	
	C101	40-G deperm TA	2.2	75	2
	MC-1	40-G deperm FA	1.4	82	1
	MC-1	Reworked	1.3	90	
	MC-5	40-G deperm FA	1.1	72	1
	MC-1	Reworked	1.4	90	
	MC-5	Reworked	0.4	30	2
Plasma probe (32A1)	397	As received	72.0	64	1
	397	25-G perm	122.5	93	3
	397	80-G deperm	8.4	79	3
	397	40-G deperm TA	2.4	72	3
	438	40-G deperm FA	1.2	83	
	408	40-G deperm FA	0	—	
Plasma probe electronics (32A2)	02	As received	13.8	80	1
	02	25-G perm	32.5	96	2
	02	80-G deperm	1.1	90	
	02	40-G deperm TA	9.1	166	
	5	40-G deperm FA	3.5	84	
	6	40-G deperm FA	1.1	60	2
Plasma probe electronics (32A3)	02	As received	1.7	80	
	02	25-G perm	1.4	96	2
	02	80-G deperm	0.4	90	
	02	40-G deperm TA	0.6	116	
	5	40-G deperm FA	0.6	65	
	6	40-G deperm FA	1.4	85	2
Plasma probe electronics (32A4)	03	As received	9.6	90	1
	03	25-G perm	31.2	95	
	03	80-G deperm	1.1	76	
	03	40-G deperm TA	1.2	72	
	6	40-G deperm FA	1.7	67	
	7	40-G deperm FA	0.3	72	1

Table A-1. (contd)

B_{max} at 3 ft, γ	Measurement distance, ft	B_{max} at measurement distance, γ	B_{max} from three measured amplitudes, γ	Components of magnetic field at spacecraft magnetometer sensor, γ			Total field magnitude at spacecraft sensor, γ	Distance from hardware CG to sensor, in.	Notes
				x	y	z			
10.9	3	10.9	7.7	0.68	0.36	0.34	0.84	71	
10.0	3	10.0	9.8	−0.79	−0.10	−0.29	0.85	70	
8.0	3	8.0	8.1	0.55	0.25	0.22	0.64	71	Assembly offset on mapping turntable to compensate for offset in dipole due to latching relays
7.9	3	7.9	8.0	−0.68	−0.02	−0.18	0.70	70	
11.0	3	11.0	11.0	0.81	0.34	0.26	0.92	71	
10.7	3	10.7	10.8	−0.87	−0.11	−0.29	0.92	70	
11.1	3	11.1	11.1	0.82	0.34	0.26	0.92	71	
9.9	3	9.9	10.0	−0.77	−0.10	−0.29	0.83	70	
11.5	3	11.5	11.7	−0.72	0	−0.48	0.87	70	
10.7	3	10.7	10.7	1.01	0.18	0.09	1.03	71	
11.0	3	11.0	10.7	0.32	0.21	0.61	0.72	71	Slight offset in dipole
10.9	3	10.9	10.4	0.28	0.34	0.59	0.74	71	
10.7	3	10.7	10.6	0.40	0.17	0.55	0.70	71	
10.6	3	10.6	10.3	−1.16	−0.08	0.03	1.16	70	
10.4	3	10.4	10.4	−1.07	0.09	−0.07	1.08	70	
12.8	2	43.1	40.1	−0.01	2.01	−0.84	2.18	65	
5.1	2	17.4	17.0	0.06	0.63	0.11	0.64	65	
4.9	2	16.5	16.3	−0.08	−0.61	−0.09	0.62	65	
0.5	2	1.6	1.3	−0.01	−0.03	0.05	0.06	65	
0.6	2	1.9	1.9	0	0.08	−0.05	0.09	65	
0.4	2	1.2	1.2	0.03	−0.03	0.04	0.06	65	Not simple dipole
0.3	2	1.2	1.2	0	−0.04	0.03	0.05	65	
0.3	2	1.0	0.7	0.04	0	0.02	0.04	65	Not simple dipole
0.4	2	1.3	1.3	0	−0.05	0.04	0.06	65	
0.1	2	0.3	0.4	0.01	0.01	0	0.01	65	Excessively noisy mapping
18.8	3	18.8	17.8	0.85	−0.74	0.63	1.29	84	
32.1	3	32.1	32.0	−2.32	0.96	−0.34	2.53	84	
2.2	3	2.2	2.2	−0.16	0.06	0.01	0.17	84	
0.6	3	0.6	1.0	−0.05	0.01	0.01	0.05	84	
0.3	2	1.1	1.2	−0.02	−0.01	0.01	0.02	84	
0	2	0	0	0	0	0	0	84	
3.6	1.5	28.9	27.2	0.14	−0.20	0.16	0.29	81	
8.5	1.5	68.0	67.4	0.05	0.55	−0.42	0.69	81	
0.3	1.5	2.4	2.5	−0.01	−0.02	0.01	0.02	81	
2.4	1.5	19.1	19.3	−0.06	−0.11	−0.05	0.13	81	
0.9	2	3.1	3.1	−0.08	0.01	0.01	0.08	81	
0.3	2	0.9	0.8	0	0.02	−0.01	0.02	81	
0.4	1.5	3.5	3.5	−0.01	−0.02	0.02	0.03	82	
0.4	1.5	3.0	3.0	−0.01	0.02	−0.01	0.02	82	
0.1	1.5	0.8	1.0	−0.01	0	0	0.01	82	
0.2	1.5	1.2	1.3	−0.01	−0.01	0	0.01	82	
0.2	1.5	1.3	1.3	0	−0.01	0.01	0.01	82	
0.4	1.5	2.9	2.8	0	0.03	−0.01	0.03	82	
2.5	1.5	20.0	20.0	0.12	−0.14	0.08	0.20	83	
8.2	1.5	65.4	63.9	−0.51	−0.34	0.22	0.65	83	
0.3	1.5	2.4	2.3	−0.02	0	0.01	0.02	83	
0.3	1.5	2.5	2.3	−0.01	−0.01	0.02	0.02	83	
0.4	1.5	3.5	3.4	−0.01	−0.02	0.02	0.03	83	
0.1	1.5	0.6	0.8	0	0	0	0	83	

Because the 40-G demagnetization was performed both as part of the type approval evaluation and also as the treatment of flight approval hardware, these two operations are distinguished by TA and FA in the third column.

The dipole moment, which was determined by calculation, is given in the fourth, fifth, and sixth columns. The magnitude is given in the fourth column in CGS units and the orientation is specified by θ and ϕ components of the spherical coordinate system. The $\theta = 0$ coordinate is in the spacecraft + Z direction, which is the direction toward the sun when the spacecraft is attitude-stabilized and parallel to the low-gain antenna waveguide in Figs. 1 and 2. The low-gain antenna is at the − Z end of the waveguide. The solar panels lie in the spacecraft XZ plane with the Bay 1 solar panel in the + X direction. The spacecraft coordinate system is a right-hand system. The ϕ coordinate in the fifth column is measured from 0 to 180 deg, while the ϕ coordinate in the sixth column is the angle between the plane containing the spacecraft Z axis and the dipole moment vector and the spacecraft XZ plane, measured clockwise from the XZ plane from 0 to 360 deg when looking in the + Z direction.

The seventh column is the extrapolated value of the maximum field component of the dipolar magnetic field at 3 ft from the approximate geometric center of the hardware being mapped. This distance, by common usage, has become a mapping standard. The maximum radial field occurs on the axis of the dipole. The eighth column lists the mapping distance from the approximate geometric center of the hardware to the mapping magnetometer probe. The ninth column is the maximum radial component of the dipolar magnetic field at the measurement distance specified in the eighth column, as determined by calculation from the amplitudes and angles obtained from two of the three mappings having the greatest amplitude. The tenth column gives the maximum radial field magnitude as determined by taking the square root of one-half the sum of the squares of the maximum field amplitude determined in each of the three orthogonal mapping planes.

The eleventh through thirteenth columns give the X, Y, and Z components, respectively, of the dipolar magnetic field of the hardware at the relative position of the spacecraft science magnetometer sensor in spacecraft rectangular coordinates. The fourteenth column is the total field magnitude at the spacecraft sensor position and is obtained by taking the square root of the sum of the squares of the components in columns 11 through 13. The fifteenth column is the distance from the approximate CG of the hardware when installed on the spacecraft to the center of the spacecraft science magnetometer sensor, and is used in computing the component values listed in columns 11 through 13. The last column primarily contains notes on the nature of the mapping obtained. In general, a quadrupole in this column indicates that the mapping deviates noticeably from a pure sine curve in that double humps are evident. An offset dipole is indicated where this is apparent in the XY plotter data (Ref. 5).